AN ABSTRACT OF THE THESIS OF

JUKCHAI BENJARATTANANON for the degree of Master of Science in Industrial Engineering presented on August 5, 1998. Title: Sources of Weld Strength Variability in Capacitor Discharge Welding.

Redacted for Privacy

Abstract Approved: _____

Brian K. Paul

Capacitor discharge welding (CDW) is a rapid solidification joining process under the influence of one-dimensional thermal gradients. Although CDW is useful for joining small parts and dissimilar metals, CD welded joints have a large variability in weld strength. CDW is not widely accepted because of a lack of automated process control. Studying the sources of variability in the CDW process can guide the automation of CDW. Therefore, the objectives of this study were to investigate sources of variability that affect weld strength and to generate a model to predict the weld strength variability in CDW. The source of variability was investigated by using screening experiments. Four different materials, stainless steel, Nitronic 50 Steel, copper, and low oxygen copper (C101), were selected to represent various levels of thermal conductivity and absorbed gas content. Thermal conductivity, percentage of gas content absorbed, diameter, and welding time were treated as the independent variables while the dependent variables were the standard deviation of CD weld strength as a percentage of base material strength and the mean of CD weld strength as a percentage of base material strength. A screening experiment and a statistical analysis of the data were used to develop a predictive model

of the weld strength variability in CDW. Electron photomicrographs of weld fracture surfaces and dynamic current and resistance curves for each welding cycle were used to support conclusions from the statistical analysis. Conclusions of this study are that thermal conductivity and absorbed gas content do have a significant influence on weld strength variability in CDW.

Sources of Weld Strength Variability in Capacitor Discharge Welding.

By

Jukchai Benjarattananon

A THESIS

submitted to

Oregon State University

in partial fulfillment of
the requirements for the
degree of

Master of Science

Presented August 5, 1998

Commencement June, 1999

Master of Science thesis of Jukchai Benjarattananon presented on August 5, 1998

APPROVED:

Redacted for Privacy

Major Professor, representing Industrial Engineering

Redacted for Privacy

Chair of Department of Industrial and Manufacturing Engineering

Redacted for Privacy

Dean of Graduate School

I understand that my thesis will become part of the permanent collection of Oregon State University libraries. My signature below authorizes release of my thesis to any reader upon request.

Redacted for Privacy

Jukchai Benjarattananon, Author

ACKNOWLEDGEMENT

First of all, I would like to deeply express my heartfelt gratitude to my professor, Dr. Brian K. Paul, for his valuable guidance and assistance in every aspect during research. Secondly, appreciation is extended to Dr. Rick Wilson for his recommendations throughout the research and his participation as one of my graduate committees. I also would like to thank Dr. Edward McDowell for his interest and serving as my minor professor.

Finally, I am really particularly grateful to my parents not only for their constantly moral and financial supports, but also their perpetual encouragement.

TABLE OF CONTENTS

TABLE OF CONTENTS (CONTINUED)

TABLE OF CONTENTS (CONTINUED)

LIST OF FIGURES

LIST OF FIGURES (CONTINUED)

LIST OF TABLES

LIST OF TABLES (CONTINUED)

LIST OF APPENDICES

LIST OF APPENDIX FIGURES

LIST OF APPENDIX TABLES

Sources of Weld Strength Variability in Capacitor Discharge Welding

1 Introduction

Capacitive discharge welding (CDW) is an autogenous, rapid solidification (RS) joining process that is good for joining small geometries of hard-to-weld materials including high-strength/high-temperature alloys, intermetallic compounds, electrical contacts, ceramics, metallic glasses, metal-matrix composites, and electronic superconducting materials among others. It is anticipated that the importance of CDW will increase largely because of three factors. First, the number of the new materials requiring RS joining methods continues to increase. Second, modern designs continue to demand greater performance while reducing weight and cost. Designers are increasingly seeking to combine dissimilar metals to meet these requirements. At the same time, designers are striving for improved product manufacturability including the elimination of fasteners in favor of alternate joining methods. Third, CDW is environmentally benign when compared with brazing and soldering methods and CDW produces much higher quality welds than resistance spot welding processes. Based on Department of Commerce data (Census of Manufacturers 1987), it is estimated that over 2.8 billion brazing, soldering, or spot welding joints were made in the U.S. in 1987 that could have used CDW.

Although CDW has many advantages compared with other joining processes, very little automated process control has been applied to CDW. It is generally recognized that weld quality in resistance welding processes, such as spot welding and CDW can be highly unpredictable. As an example, there are typically about 2,000 to 5,000 spot welds

in every passenger car. However, because of a lack of confidence in the quality and consistency in the welds, a typical automobile has up to 30% more welds than required to maintain its design requirements (Faitel, 1995). It is the objective in this study to investigate the sources of weld strength variability in CDW to determine if and what type of automated process control would be beneficial to the processes.

1.1 Variability in Resistance Welding

Spot welding was invented in 1877, and since then there have been many studies performed to understand the physics of this process. Some studies have revealed the sources of variability in the spot welding process. One of the causes of quality variation in this process is electrode wear because the shape of the electrode affects the specimen contact stress and surface resistance (Change et. al., 1977). In Fukushima and Kasugai's (1990) study of welding of Fe-Si-B amorphous alloy foil, amorphous foil was welded using capacitive discharge spot welding. Their research showed that variability of joint strength decreased as the charging energy in capacitor banks increased. In addition, the quality of the base metal influenced the variability of joint strength. As Johnson (1977) reported, variation of quality in spot welding can be presented due to voltage fluctuation, cable deterioration, electrode wear. Moreover, Kliped (1988) revealed that thickness of the sheet, the weldability of materials, and the size and the number of welds are the factors affecting the tensile strength in spot welding. Moreover, there is variability in weld quality due to changing impedance of the weld circuit, and the shunting effect (Cho and Chan, 1985).

Weld strength variability is an issue in other resistance welding processes such as percussion welding as well. However, very few studies have been conducted investigating weld strength in percussion welding processes such as CDW. The subject of this thesis is the study of weld strength variability in the initial gap method of low-voltage CDW.

1.2 Welding Automation

Many past research studies have been accomplished to control the variation in weld quality, because an increase in the reliability of weld quality leads to a reduction in production cost. According to Morgan-Warren (1974), in the study of the arc stud welding control system, the control of energy input and weld force can insure the reliability in the arc stud welding process. In addition, the welding institute invented the voltage spot weld correction weld system to use in mass production. This system ensures weld quality by reducing variation due to voltage fluctuation and electrode wear (Johnson, 1977).

Automated welding is another alternative to reduce variability in the welding process. Welding automation has been known since the 1920's, although automation has been difficult to implement in welding processes (Cary, 1985). Automated welding plays an important role in the welding industry due to the possibility of obtaining higher productivity and maintaining consistent product quality. According to Lanstorm (1937), output of a spot welder can be increased from 75 spots per minute to 200 spots per minute by putting automatic control to the welder. Furthermore, many percussion welding automation systems have been developed to improve weld quality including a

percussion welding system developed by Quinlan (1955) involving a double gun mechanism, the Bitterman stud welder, and the Nelson stud welder developed by TRW. In addition, since the large part of the cost of welding processes is the labor cost, another benefit of welding automation is the cost reduction caused by using a full or partial mechanized system instead of a manual system (Norrish, 1992).

According to the Census of Manufactures (1987) data, CDW can replace some types of welding such as soldering, brazing, or resistance spot welding, because of its application (See 2.3.4 advantages and 2.3.5 limitations of CDW). Although CDW has many advantages compared with resistance welding, soldering, or brazing, CDW is not widely accepted in industries due to weld strength variability.

1.3 Potential Sources of Variability in CDW

In the CDW process, there are many parameters that may be the source of weld strength variability. Some of these parameters are discussed in more detail below. Thermal conductivity is material-dependent since different materials have different levels of conductivity. It is expected that thermal conductivity affects the variability of the CD weld strength because of heat conduction in the base material. In the CDW process, after the surface of the electrodes are heated by the arc, the majority of the energy is axially conducted along both electrodes. As a result, the cooling rate of the welded joint depends on the thermal conductivity of the material welded. The higher the thermal conductivity of the base metal, the higher the cooling rate of the CDW process. However, if the process has too high of a cooling rate, the molten surface of the electrodes will solidify

before the electrode makes complete contact, and then, the welded joint cannot make complete fusion.

As Ramirez et al. (1994) reported, the cause of porosity in weld joints is the dissolved gas in the base metal that comes out of solution during the welding process. Porosity also has an adverse impact on the strength of a welded joint since it decreases weld area. So the more porosity, the lower the strength of the welded joint. Therefore the percentage of gas content in a material may be one of the parameters to affect variability in weld strength.

Another parameter that may cause variability in the CDW process is the welding time. As Wilson and Hawk (1994) reported, weld strength is maximized as Tw approaches 2RC where R is the total circuit resistance and C is the capacitance. This has been found independent of electrode material. This suggests that there exists an optimal weld condition achieved by the balance between process kinematics and capacitive discharge rate.

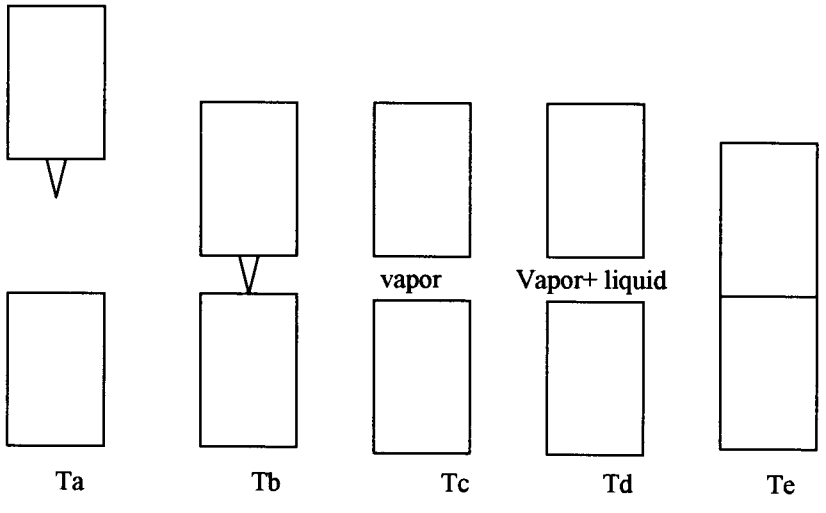

Figure 1.1. Physical process.

Figure 1.1 shows the physical process of CDW. Welding time begins when the initial contact is made at time Tb and ends when the electrodes contact at time Te. Consequently, welding time is defined as follows

$$Tw = Te - Tb \tag{1.1}$$

where Tw is welding time; Te is the time when electrodes make complete contact; and Tb is the time when electrodes make initial contact. In addition, welding time can be estimated by using the following equation:

$$Tw = (L+b) / \sqrt{2gH} \tag{1.2}$$

where Tw is the welding time; b is the melt back distance; L is the tip length; H is the drop height; and g is acceleration due to gravity. When the welding time is too fast or too slow, weld defects occur (see description in 2.3.6 CD-welded defects).

Another potential source of variability is the arc mode. According to the *Welding Handbook* (1991), " the welding arc can be defined as a particular group of electrical discharge that are formed and sustained by the development of gaseous conduction medium." The welding arc is considered a refractory arc, when the welding arc is stable. On the other hand, the welding arc is a cold-cathode arc, when it is intermittent or continuously unstable due to the alternating directional flow of current or the turbulent flow of the conducting gas medium. It is assumed that the variability of strength in CDW may be affected by the arc mode presented at the time of welding. Under cold cathode conditions, the arc randomly moves across the faying surfaces creating hot and cold regions. If this is an effect in CD weld strength, then weld strength variability should be less for smaller diameters.

1.4 Summary

In this study, thermal conductivity, percentage of gas content in base material, diameter, and welding time, will be investigated as sources of weld strength variability in CDW. Chapter 2 will present some kinds of weld defects, and the background of CDW. Methods and materials will be presented in Chapter3. Chapter 4 is the result and analysis section. Finally, conclusions will be made in Chapter 5.

2.Literature Review

2.1 Welding Defect

Welding defects include cracks, inclusions, and voids among others. Each of these will be explained in more detail below.

2.1.1 Weld cracking

The restrained contraction of a weld during cooling sets up tensile stress in the joint and causes cracking (Lancaster, 1987). Cracking can occur either during the fabrication or after the operation is completed. Macrocracking is a specific term for cracking observed by the naked eye, while microcracking is used to specify cracking observed by special equipment, such as a microscope. However, cracking can take place in the weld joint, and in the base metal adjoined to it, especially in the heat affected zone (HAZ). Additionally, cracking can be classified as hot or cold cracking: hot cracking occurring during solidification and cold cracking occurring in the base metal or HAZ.

One of the causes of cracking is the residual stress: the stress remaining in the structure or member as a result of the thermal or mechanical treatment or both (Cary, 1979). The stiffness or rigidity of the weld metal is one of the causes of restraint. The higher the restraint nature of the material of a weld, the less chance of movement of the weld in the weld joint. Cracking can happen, if the ductility of the weld metal is inadequate. During cooling, when the weld metal shrinks, cracking will occur, if the residual stress increases beyond the yield strength of the material. In addition to this, in the steels rapid cooling of the weld joint causes cracking due to the martinsitic

transformation. This problem can be solved by preheating the parts before welding because preheating can decrease the cooling rate of the material being welded and post weld heat treatment.

Another cause of cracking is the alloy composition. During welding of a high carbon or high alloy base material. Segregation of high melting elements from low melting element can reduce weld strength and ductility. Consequently, the weld metal consists insufficient ductility can cause less plastic deformation, and then cracking can take place. Using a more ductile weld metal and decreasing the cooling rate of the weld can solve this problem.

2.1.2 Inclusion

As Giachino et al. (1968) report, " Inclusions are impurities which are formed in a molten puddle during the welding process." Inclusions act as stress risers in the welding joint and can initiate cracks. Generally, slag inclusions are the most common type of inclusion. In this type, a nonmetallic solid material is entrapped in the weld metal or between the weld metal and base metal. Flux inclusions are another type of inclusion. Fluxes found from electrodes are entrapped in the weld metal or between the weld metal and base metal. In general, both types of inclusion formed geometries with rounded ends, not sharp cornered ends. Consequently, inclusions are not as serious a problem as cracks.

With oxide coated metals, there is a greater potential for oxide inclusion to occur. For example aluminum oxide on the surface of aluminum can be entrapped in the

deposited weld metal, so it is necessary to take proper precautions and clean the weld metals. (Cary, 1979)

2.1.3 Void

Porosity refers to the formation of tiny pinholes, generated by atmospheric contamination. Porosity is caused by gases that are present in the surrounding in the base metal, which are trapped in the molten during the solidification process (Cary, 1979). The causes of porosity include the following:

- High sulfur in the base metal.
- Inclusion of gas from the atmosphere such as oxygen or nitrogen.
- Hydrocarbons on the surface of the metal such as paint, water, or oil.

Porosity can be considered to be of two types: surface porosity and subsurface porosity. Surface porosity can be observed by the naked eye (without any non-destructive inspection technique). On the other hand, subsurface porosity must be detected by using a non-destructive inspection technique.

In comparison to cracks, the defect due to porosity is less serious because the porosity cavities are generally rounded ends and they do not propagate as easily as cracks. (Cary, 1979)

2.2 Heat-Affected Zone (HAZ)

During the joining of the base metal by welding, the base metal is heated to its melting point and then cooled. The microstructure and properties of the metal in the area

adjoining to the weld are altered because of a severe thermal cycle. This area is generally called the heat-affected zone (HAZ) (Irving, 1995). The HAZ is present in all welding operations. The width of the HAZ is a function of the material and the welding process . In the HAZ, increasing temperatures beyond critical point may affect the structure of the joint by causing grain growth and grain recrystallization adjacent to the weldment.

The following are some effects of the alloy element has on the HAZ:

1. Solid state alloys are made by adding similar alloy which generally increase the strength of pure metal. The alloy element can obstruct the movement of dislocations, and this makes the metal stronger. Thermal cycle in the HAZ causes little change in the mechanical characteristics of materials like aluminum and copper.

2. Strain-hardened materials are alloys that have gone through the strain hardening process like rolling where the alloy is strengthened and toughened by cold working, a process of deforming metal below the recrystallization temperature by hammering, rolling, drawing, and pressing (Giachino, et al., 1968). However, when cold worked material is recrystallized during the welding cycle, the material is heated beyond the recrystallization temperature the grains grow and the fracture toughness decreases in the HAZ.

3. Most nonferrous metals are strengthened by precipitation hardening. The alloy element is aggregated within the material lattice by using a heat treatment. The second phase precipitate can obstruct the movement of dislocations, and then increase the strength of the metal. Overheating the alloy results in large precipitates that are wildly spaced which are less effective in preventing dislocation movement. Like the strain-hardening alloy, metal in the HAZ is weakened.

4. Transformation-hardened alloys are the steels containing enough carbon and other alloying element such that recrystallized grains of HAZ transform to martensite on cooling. Grains adjacent to the fusion line recrystallize from austenite to martensite as the weld temperature drops. Hard, brittle, high carbon martensite leads to hot cracking, when welds contain dissolved hydrogen and residual stress.

2.3 Capacitor Discharge Welding (CDW)

According to *the Welding Handbooks* (1991), there are three different types of capacitor discharge welding: initial contact, initial gap, and draw arc. In this thesis, CDW is operated by using the initial gap method. Initially, there is gap between electrodes. The cathode is released and continuously moves toward the anode under gravity to make a complete weld joint.

Since the late 1980's, CDW has been investigated as a rapid solidification welding process even though CDW generally has been applied to stud welding (Venkataraman and Devletian, 1988). The CDW process can relieve the problem of losing metastable crystalline structure, grain refinement, and reduced segregation in joining rapidly solidified crystalline materials. Moreover, CDW is effective for joining dissimilar metals. Unlike brazing and soldering, CDW doesn't require fillers containing of chloride, fluoride, or lead; as a result, environmental side effects are decreased (Wilson et al 1994).

In 1987, Devletian studied the weld microstructure of a Si/Al metal matrix composite, which was joined by using the CDW process. Devletian's study showed that there was less porosity in the weld joint using CDW versus other high heat input

processes such as Gas tungsten Arc Welding (GTAW). CDW, therefore. was appropriate for welding metal matrix composite properties. In addition, Baeslack III, et al. (1988) revealed that an Al-Fe-Ce alloy could be welded by using the CDW process. There was no porosity presented due to the rapid solidification properties of CDW.

Venkataraman and Devletian (1988) set up an experiment to study the process parameters in CDW in order to forecast the weld cooling rate while solidification takes place. Three types of stainless steel, 304, 316 and 318 stainless steel, were used as specimens in this study. The followings are the results from their experiment

- Increasing drop height and decreasing ignition tip length lead to reduced weld thickness;
- Decreasing voltage can also decrease weld thickness;
- Ignition tip length and drop height were the most significant parameters in controlling rapid solidification;
- Drop weight is an insignificant parameter;
- Decreasing arc time can decrease weld thickness;
- Average weld thickness is a linear function of the square root of arc time;
- The most significant parameters in welding time are drop height and ignition tip length.

Also, an equation of power density was developed by Venkataraman and Devletian (1988). This equation was used to quantitatively explain the effect of the process parameters on cooling rate during welding:

$$P = CV^2/(4at) \tag{2.1}$$

where t is arc time; C is capacitance; V is voltage, and a is weld cross section area.

In 1991, Wilson developed a welding time model. This model shows that ignition tip length and drop height are the significant parameters in welding time. Subsequently, dissimilar metal joining was conducted by Wilson and Hawk (1994). Aluminum tube and steel shells were employed in this study.

Wilson et al. (1993) used ultrahigh speed photography to study the heat flow characteristics of the CDW process by using a $Fe_{76}Al_{24}$ intermetallic alloy as a specimen. They found that the metal particles moved away from the weld due to the plasma jet during the process. In addition, the CDW process can be determined to be one-dimensional due to heat flow process.

Because of the nonequiliblium nature of high nitrogen stainless steel, nitrogen, a strengthening agent, will be lost in the fusion zone and the HAZ during the welding process. Hence, it is hard to weld high nitrogen stainless steel. Simmons and Wilson (1996) studied the joining of high nitrogen stainless steel by CDW.

As Wilson et al. (1993a) reported, "Capacitor Discharge Welding (CDW) is a rapid solidification joining process capable of a cooling rate greater than 10^6 K/s. Experience has shown that welding tip length, capacitance, voltage, and electrode separation (i.e. drop height) are the important factors controlling the CDW process."

2.3.1. Physical Process

According to Wilson et al. (1993), the schematic procedure of the CDW cycle is shown in Figure2.1. In Figure 2.1a, the cathode is in the initial position at a drop height (H), connected to a full capacitor bank with capacitance (C), and infinite resistance circuit. Initial contact between the cathode and anode via an ignition tip is shown in

Figure 2.1b. At this point, the capacitor bank is discharged. Figure 2.1c shows that the ignition tip vaporizes forming an arc between the electrode surface. As the arc plasma spreads out plasma and molten particles are expelled due to the magnetic field induced by the current flow (Figure 2.1d). Finally, Figure 2.1e shows a completed welding joint.

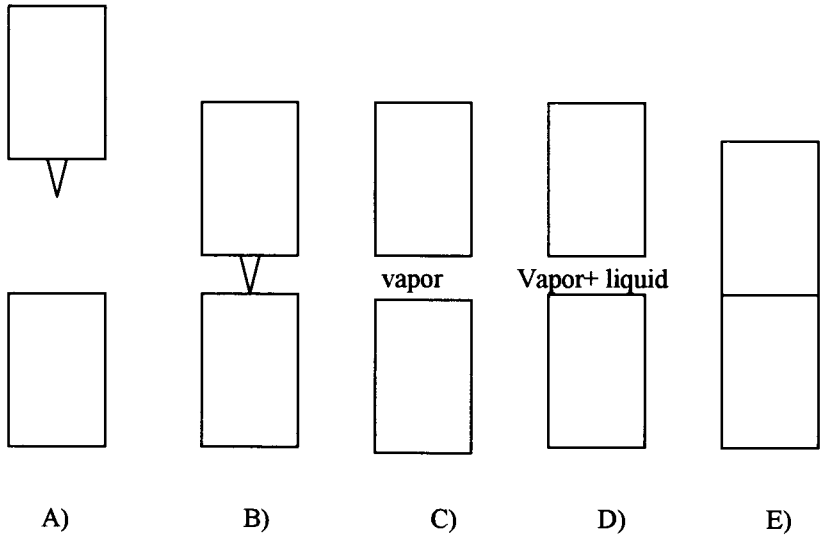

Figure 2.1. Physical process.

2.3.2 Process Thermodynamics

In the CDW process, there are many parameters involved in controlling weld quality. Heat input and welding time, however, are the most significant factors in controlling CDW conditions. By optimizing all parameters in both factors, better weld joint quality can be developed.

According to Wilson (1993), the energy input into a CD-weld joint must be high enough that the electrode tip is completely molten and there is melting across the entire surface.

The first law of thermodynamics has been used to determine the minimum heat input in the CDW process:

$$\Delta H_v = Mc_p \Delta t_v \tag{2.2}$$

where Δt_v is the material boiling temperature in degrees Kelvin; M is the mass of the affected metal; and c_p is the specific heat of material.

Also, the energy required in melting material can be determined by using the enthalpy equation:

$$\Delta H = mh \tag{2.3}$$

where ΔH is the total enthalpy; m is the total mole of affecting metal; and h is the specific enthalpy.

The energy required in the CDW process is calculated from the combination of energy required to expel flash (H_{flash}) and the energy required to form the weld (H_{weld}):

$$\Delta H_{total} = \Delta H_{flash} + \Delta H_{weld.} \tag{2.4}$$

Multiplying by an efficiency factor can compensate energy loss else where in the circuit due to extraneous resistance. The energy stored in the capacitor bank can be determined by the following equation:

$$E = \tfrac{1}{2} CV^2 \tag{2.5}$$

where E is the energy stored in the capacitor bank; C is capacitance; and V is voltage.

Setting equation 2.4 and 2.5 equal to each other provides a governing equation for CDW.

2.3.3 Process Kinematics

The parameters that are significant for the CDW process are voltage (V);

capacitance (C); welding tip (L); and electrode separation (i.e. drop height (H)). However, the tip length and drop height are important for welding time (Simmons and Wilson, 1996) (see Figure2.2).

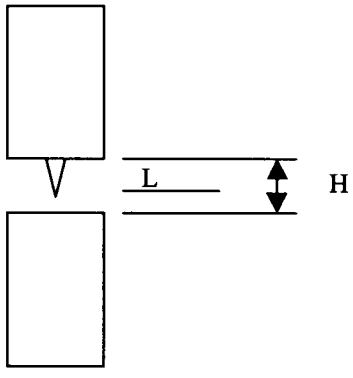

Figure 2.2. Process Kinematics.

Dropping the cathode to the anode with height (H) and acceleration due to gravity (g) discharges the DC capacitor.

Welding time starts when the ignition tip of the cathode touches the anode and ends with the consummation of the weld. With reference to figure 2., we know that the distance traveled during this time is the ignition tip length. The velocity at impact, V, (equation 2.7) can be derived from the conservation of energy law (equation 2.6):

$$mV^2/2 = mgH \tag{2.6}$$

$$V = \sqrt{2gH} \tag{2.7}$$

Consequently, welding time can be approximated by

$$Tw = (L+b)/\sqrt{2gH} \tag{2.8}$$

where Tw is the welding time; b is the melt back distance; L is the tip length; H is the drop height; and g is acceleration due to gravity.

According to Wilson and Hawk (1994), the metallurgical properties of a welding joint depends on welding time. For instance, too long of a welding time causes solidfication of faying surface prior to the electrodes meeting. Therefore the process kinematics must be coordinated with the capacitor discharge. The RC time constant and welding time are characteristic factors for strength in a weld joint. The RC/Tw ratio is significant since this ratio concerns the relationship between energy delivery time and mechanical electrode positioning time. As explained weld defects occur when solidification takes place before the electrodes are brought in contact. Also, weld defects can take place if RC time constant is considerably longer than the welding time since (i.e. welding time is too short) there is inadequate energy to fuse the outer surface of the specimen. Wilson and Hawk (1994) showed that the optimal welding time for maximizing weld strength occurs around 2RC. This relationship has been shown to be material independent.

2.3.4 Advantages of CDW

CDW is a rapid solidification process that provides good weld strength due to:

- The welding process can affect only a small volume of the part;
- A fine-grained structure can be formed due to its rapid cooling rate;
- Filler is not required in this process, so the strength is not changed due to the composite material.

High heat input from conventional welding processes such as resistance spot welding affects the microstructure of the base material. Especially, in the fusion zone and heat-affected zone, grain growth and recrystallization can be developed. In addition, porosity due to material overheat also can occur. On the other hand, CDW can alleviate weld defects caused by high heat input. Generally, the fusion zone due to a CDW process is about 50 μm thick, and the heat-affected zone paralleling to the centerline is small if not negligible.

Furthermore, in CDW, oxide moves away from the weld joint with the expanding arc plasma. On the other hand, in resistance spot welding, oxide cannot be removed from the joining region, so inclusions are formed.

Reducing environmental emissions is one of the benefits of the CDW process because the CDW process doesn't require fluxes. Fluxes are utilized to eliminate any forms of oxide on the surface of a joining region, which obstruct a flow of filler material. Typically, toxic fumes will occur during soldering, brazing, or any welding processes using fluxes because flux ingredients usually are fuse borax, boric acid, fluoride, and chloride.

Also, high heat input welding processes have significant amount of elementary diffusion, which can create small amounts of deleterious intermetallic phase in joining dissimilar materials because of rapid solidification. CDW can be used for joining dissimilar materials (Wilson and Hawk, 1994). Furthermore, the fusion zone (FZ) and the heat-affected zone (HAZ) from CDW are quite small compared with other welding processes.

2.3.5 Limitations of CDW

As we can see, the CDW process has many benefits in comparison to the high heat input welding processes. However, CDW has limitations as well. The size of part to be welded is a limitation because of the finite energy contained in the capacitor bank. Consequently, CDW is appropriate to weld small parts. The ignition tip length is also a problem in the CDW process. To control welding time, precise ignition tip length is required for each particular CDW. In addition, the part to be welded must be an electrically conductive substance (Wilson and Hawk, 1994).

2.3.6 CD-Weld Defects

Welding defects in CDW can be due to a number of factors. The ratio of the welding time to the RC time constant of the circuit can significantly affect weld quality is in CDW. According to Wilson and Hawk (1994), the optimum welding time obtaining maximum weld strength is:

$$Tw = 2RC \tag{2.9}$$

where R is total circuit resistance and C is capacitance. If Tw is less than 2RC, a weld defect known as arc shorting will occur because there is inadequate energy to melt the surface of the specimen before the electrode come together. If energy input is insufficient due too low voltage or too low capacitance, arc shorting will be occurred as well. On the other hand, when Tw is longer than 2RC, pre-solidification takes place where the faying surfaces solidify before coming together.

In addition to welding time, the shape and geometry of the joining region surface significantly affects the weld quality in the CDW process because the ordinary CD weld

is only 100μm. Large surface asparities on the electrodes can causes incomplete contact in the finished product. A smooth surface free of tool marks is required for complete contact. A rough surface can cause a void in welds because there is inadequate energy to melt on the asparities in the rough surface. Furthermore, the small bevel angle of the surface is necessary in ventilating metal vapor and plasma.

3. Methods and Materials

3.1. Overview

To investigate the parameters that affect CD weld strength and variability of weld joints, four kinds of materials (low oxygen copper (C101), copper, stainless steel and Nitronic 50 steel) were used in the screening experiment. Four different independent variables were chosen: thermal conductivity, percentage of gas content in material, weld diameter, and welding time. Reasons for choosing these variables are given in chapter 1. Ninety-six observations were randomly run to eliminate bias in the experiment. Then, the strength of the welded joint was tested by using an Instorn tensile test machine.

After collecting the data, it was analyzed by a statistical technique to generate the mathematical model. This model predicts the trend effected by the significant variables. Moreover, magnesium and mild steel were used to validate the statistical model generated from data.

3.2 Factorial Design

In this study, the independent variables that were investigated were thermal conductivity, percentage of gas content in the material, and weld diameter with 2 levels, and welding time with 3 levels. Consequently, a complete replicate for this experiment requires (2 X 3 X 2 X 3) 24 observations. Since one of the dependent variables in this experiment is variability, four replicates were run for this experiment. This means that 96

observations were conducted. All data were arranged into the following codes based on material type, welding time and weld diameter: MXX

There are 2 digits behind letter M. The first digit stands for type of material used in the screening experiment, where 1 is stainless steel; 2 is low oxygen copper; 3 is Nitronic 50 steel; 4 is copper; 5 is magnesium; and 6 is mild steel. Moreover the second digit behind word M stand for level of diameter and welding time as explain below:

1 is level -1 of diameter and level –1 of welding time.

2 is level -1 of diameter and level 0 of welding time.

3 is level -1of diameter and level 1 of welding time.

4 is level 1 of diameter and level –1 of welding time.

5 is level 1 of diameter and level 0 of welding time.

6 is level 1 of diameter and level 1 of welding time.

For example, M16 is stainless steel at level 1 of diameter and level 1 of welding time.

Each code has 4 observation except code M25 (data in code M25 contains only 3 observations due to an error in data collection). The standard deviation and mean were calculated. The following table (Table3.1) shows the screening experiment design. Subsequently, strength values of each base material were used to normalize standard deviation and mean data.

Table 3.1. Factor screening experiment for one replicate.

Material	Code	Out Gassing	Thermal Conductivity	Tw	Diameter
Stainless Steel	M11	-1	-1	-1	-1
	M12	-1	-1	0	-1
	M13	-1	-1	1	-1
	M14	-1	-1	-1	1
	M15	-1	-1	0	1
	M16	-1	-1	1	1
Low Oxygen Copper	M21	-1	1	-1	-1
	M22	-1	1	0	-1
	M23	-1	1	1	-1
	M24	-1	1	-1	1
	M25	-1	1	0	1
	M26	-1	1	1	1
Nitrogen steel	M31	1	-1	-1	-1
	M32	1	-1	0	-1
	M33	1	-1	1	-1
	M34	1	-1	-1	1
	M35	1	-1	0	1
	M36	1	-1	1	1
Copper	M41	1	1	-1	-1
	M42	1	1	0	-1
	M43	1	1	1	-1
	M44	1	1	-1	1
	M45	1	1	0	1
	M46	1	1	1	1

3.3 Research Design

After developing the factorial design, all conditions of each run must be set up. In order to determine initial conditions, it was decides that welding condition were needed for each material that would allow strength of the CD-welded joint to reach 80 % of the base metal strength for five consecutive welds. Consequently, conditions of each observation were optimized before starting the experiment.

3.3.1 Optimization Condition

Weld strength of a CD-welded joint can reach maximum strength by balancing kinematics and capacitor discharge conditions with the thermal cycle of the process. As discussed previously, welding time is a kinematics property, and energy stored in capacitor bank is related to a thermodynamics property in the CDW process. Optimum conditions of both properties influence the good quality in a CD-welded joint. As a result, to investigate variability in weld strength and reduce the noise as low as possible, the welding time and energy stored in the capacitor bank must be optimized. For any particular electrode, voltage was determined as a function of weld energy and capacitance according to the following equation:

$$E = CV^2/2 \tag{3.1}$$

$$V = \sqrt{(2E / C)} \tag{3.2}$$

In a particular material, if the capacitance was changed, voltage was also changed to maintain constant weld energy stored in the capacitor bank. Besides the voltage, welding time was also optimized. Moreover, to reach maximum strength, both welding

time and energy stored in the capacitor bank must be optimal. Varying drop height and tip length was done for optimizing welding time based on kinematics capacitor discharge equations. Also, voltage was varied at C = 0.07 μF for optimizing the heat input to material. The following table is the optimum condition for each material.

Table 3.2. Optimum conditions of each material

Materials	Capacitance (Farads)	Voltage (Volts)	Energy (Joules)	Tip Length (Inches)	Drop Height (Inches)	Welding Time (ms)
Copper	0.07	104.6	380	0.020	1.06	0.00078
Low Oxygen Copper	0.07	97.1	330	0.020	1.06	0.00078
Stainless Steel	0.07	75.6	200	0.020	0.89	0.00085
Nitronic 50 steel	0.07	75.6	200	0.020	0.89	0.00085

3.3.2 Varying Welding Time

To investigate variability in the weld strength of a CDW-welded joint, all external variability or noise should be minimized. This means that there should be optimum conditions for each welding time. According to past experiments, we know that welding time is proportional to a the total circuit resistance, and the capacitance as follow:

$$Tw = KRC \tag{3.3}$$

where Tw is welding time; K is a proportionality constant value; R is the total circuit resistance; and C is the capacitance.

According to the above equation, a constant value (K) and the arc resistance of the particular materials were unknown at the first stage. However, we can find those values from experiment. In each material, many joints were welded at different conditions. Then all the welded joints were tested to find the strength value. The condition that creates 80% or more base metal strength was used as the optimum condition (see Table2.).

Table 3.3. KR value for each material.

Materials	KR value
Copper	0.0111
Low Oxygen Copper	0.0111
Stainless Steel	0.0121
Nitronic 50 Steel	0.0121

The above table shows the KR constant value at C = 0.07 F. Optimum conditions at other C values were found. Using the following:

$$Tw_o = KRC_o \tag{3.4}$$

$$KR = Tw_o / C_o \tag{3.5}$$

$$Tw = KRC = Tw_o / C_o \tag{3.6}$$

where Tw_o is welding time at the 0.07 Farad; Tw is welding time at new capacitive; C_o is 0.07 Farad; and C is the capacitance.

3.4 Material Selection

As previously discussed the independent variables in this study are thermal conductivity, percentage of gas content in material, weld diameter, and welding time. However, weld diameter and welding time are not material-dependent. As a result, to make a decision of the material selection, we considered only the thermal conductivity property and percentage of gas content in the material. According to the design, two levels of thermal conductivity were selected. Also, two levels of percentage of gas content in materials, high and low, were selected. Thus, there are 2 levels of thermal conductivity and 2 levels of percentage of gas content in the materials. Four different materials are used in this experiment.

Table 3.4. Selection of materials.

	Thermal Conductivity HIGH	Thermal Conductivity LOW
Out Gassing HIGH	High Oxygen Copper	Nitrogen Steel
Out Gassing LOW	Low Oxygen Copper	302 Stainless Steel

Table 3.5. Percentage of nitrogen, and oxygen and thermal conductivity in each material.

Material	Nitrogen (% weight)	Oxygen (% weight)	Thermal Conductivity (0-100 C $Wm^{-1}K^{-1}$)
Low Oxygen Copper	0.0001	0.0032	397
High Oxygen Copper	0.0000	0.0443	397
302 Stainless Steel	0.0267	0.0106	37.5
Nitrogen Steel	0.7340	0.0025	42.9
Magnesium	0.0009	0.0107	155.5
Mild Steel	0.0048	0.0041	18

3.5 Specimen Preparation

In the CDW process, an ignition tip was machined onto each the cathode, so the geometry of the cathode was designed. All observations had the same size and geometry of the ignition tip. The diameter of the ignition tip was 0.020 inch, and the length of the ignition tip was 0.020 inch. The bevel angle of the cathode surface was 2 degrees. This bevel angle was designed for ventilating metal vapor and plasma.

The ignition tips of all specimens were machined by using the EMCO CNC-5 lathe. The CNC program for machining tips was designed (see appendix F). After machining all ignition, tips were measured and sorted for length using an optical microscope.

3.6 Preparation for tensile test

After welding, there were small metal particles and notches around the welded joint. These notches can cause specimen to fail prematurely during a destructive tensile test. Consequently, all notches around the welded joint were machined away before tensile test.

3.7 CDW Systems

The components of the CDW system include the DC power supply, the capacitor bank, and the data acquisition system. The current and voltage is collected by a data acquisition system and is used to compute the in-process arc.

3.7.1 CDW Circuits

The circuit of a CDW system (Figure3.1) consists of the DC power supply, capacitor banks, and a shunt resistor. The DC power supply was able to supply voltage up to 110 V with 5 amperes maximum. The DC power supply was connected parallel to the capacitor bank consisting of up to 9 of 0.01 Farad capacitors. Each capacitor bank (0.01 F) was connected in parallel with each other. A shunt of known resistance was used to help in collecting data from the experiment. This shunt was connected in a series in the circuit. The voltage drop across the shunt was collected in-process and used to calculate the in-process current. Moreover, a 30 kΩ resistor was connected in parallel to the capacitor bank for discharging the residual energy in the capacitor bank for safety.

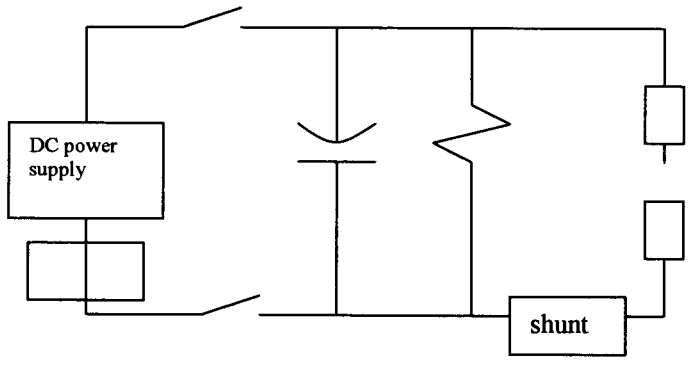

Figure 3.1 CDW circuit.

3.7.2 Data Acquisition Systems

When the ignition tip of the cathode touches the anode, the data acquisition system begins tracking the in-process current and voltage. The current increases from 0 amperes to the maximum and subsequently, decays exponentially until the electrodes are in complete contact by the end of welding time. When the electrodes make final contact, the resistance is greatly reduced resulting in a rise in the current. Figure 3.2 shows a graph of in-process current vs. time.

In addition, in-process voltage in Figure 3.3 is also collected over the welding time. When the ignition tip strikes, voltage rapidly decreases from the maximum value. After the ignition burns off the voltage increased slightly. After that, the voltage linearly decreases as the current is played out and as the electrodes get closer to one another. Finally, at the end of the welding time, the voltage potential is eliminates as the electrodes make contacts.

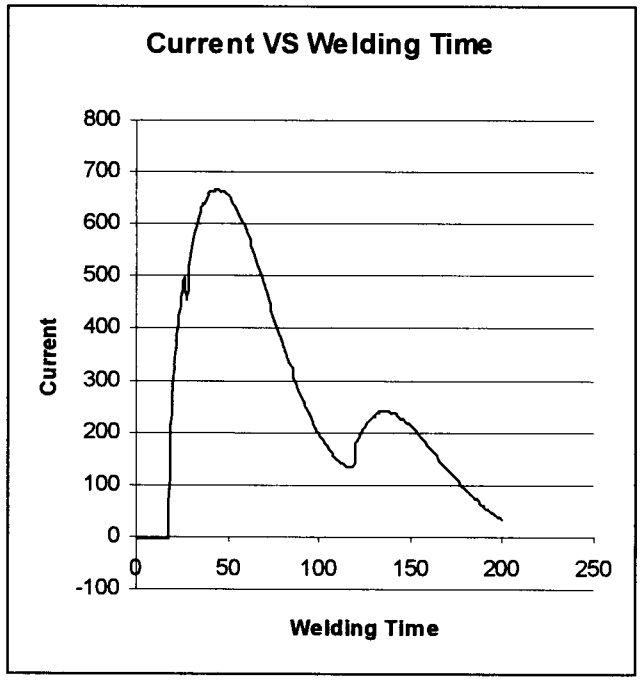

Figure 3.2 Graph from data acquisition system (Current VS Welding Time).

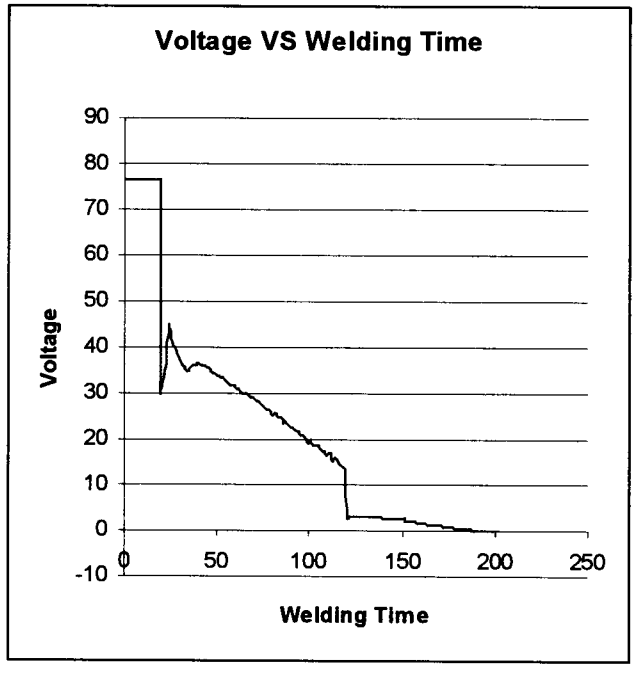

Figure 3.3 Graph from data acquisition system (Voltage VS Welding Time).

4. Results and Analysis

4.1 Overview

This chapter presents the results obtained from gage capability and the execution of the experimental design. Gage capability of a tensile test machine was measured to express the variability due to measurement error or gage variability in this machine. Subsequently, a screening experiment was run, and the data of 96 observations were collected. The observations were conducted to eliminate any bias in the screening experiment. Each code had 4 observations except code M25 (data in code 25 contains only 3 observations due to an error in data collection). The standard deviation and mean were calculated. In addition, strength values of each base material were used to normalize the data. Finally, fracture surface, weld area and multiple regression were applied to analyze the experimental data.

4.2 Gage Capability

In any experiment, the observed variability may be due to either variability in product itself or measurement error or gage variability. Variability can be expressed by the following equation

$$\delta^2_{total} = \delta^2_{product} + \delta^2_{gage} \qquad (4.1)$$

where δ^2_{total} is the total observed variance; $\delta^2_{product}$ is the component variance due to the product; and δ^2_{gage} is the component variance due to measurement error.

In this study, measurement error in the tensile test machine is expressed by the standard deviation from strength of seven specimens of brass.

Table 4.1. Gage variability in a tensile test machine.

Item	Strength (Mpa)
1	449.44
2	446.19
3	451.04
4	449.84
5	447.21
6	449.96
7	444.13
Standard deviation	2.48
Mean	448.26
Coefficient of variation	0.55%

From the Table 4.1, the standard deviation is 2.48 Mpa, that is, only 0.55 % in comparison with 448.26 Mpa of mean. The coefficient of variation represents the ratio between the standard deviation and mean. As a result, the measurement error in this tensile test machine is small.

4.3 Experimental Results

4.3.1 Weld Strength

A screening experiment was run, and the data of 96 observations were collected. These data are shown in appendix A. The observations were conducted to eliminate any

bias in the screening experiment. Each code has 4 observations except code M25 (data in code M25 contains only 3 observations due to an error in data collection). The standard deviation and mean for each condition were calculated. The following table (Table 4.2) shows the summarized data from the screening experiment where %Mean is the mean of CD weld strength as a percentage of base material strength; and %SD is the standard deviation of CD weld strength as a percentage of base material strength.

Table 4.2. Results from screening experiment.

Code	% Gas (by Weight)	Thermal Conductivity (0-100C $Wm^{-1}K^{-1}$)	Welding Time (ms)	Diameter (Inches)	Mean Strength (MPa)	SD (Mpa)	Base Material Strength (MPa)	% Mean (%)	% SD (%)
M11	0.0373	37.5	0.00085	0.125	670.17	59.65	715	93.73	8.34
M12	0.0373	37.5	0.00097	0.125	707.24	42.05	715	98.91	5.88
M13	0.0373	37.5	0.00109	0.125	732.06	57.40	715	102.39	8.03
M14	0.0373	37.5	0.00085	0.250	649.52	15.56	715	90.84	2.18
M15	0.0373	37.5	0.00097	0.250	658.97	31.39	715	92.16	4.39
M16	0.0373	37.5	0.00109	0.250	625.33	25.44	715	87.46	3.56
M21	0.0033	397	0.00078	0.125	128.01	38.24	350	36.58	10.92
M22	0.0033	397	0.00089	0.125	47.68	30.18	350	13.62	8.62
M23	0.0033	397	0.00100	0.125	157.87	142.57	350	45.11	40.74
M24	0.0033	397	0.00078	0.250	282.63	10.75	350	80.75	3.07
M25	0.0033	397	0.00089	0.250	254.79	21.42	350	72.80	6.12
M26	0.0033	397	0.00100	0.250	199.37	23.33	350	56.96	6.67

Table 4.2 (continued). Results from screening experiment.

Code	% Gas (by Weight)	Thermal Conductivity (0-100C $Wm^{-1}K^{-1}$)	Welding Time (ms)	Diameter (Inches)	Mean Strength (MPa)	SD (Mpa)	Base Material Strength (Mpa)	% Mean (%)	% SD (%)
M31	0.7365	42.9	0.00085	0.125	684.38	116.38	924	74.07	12.60
M32	0.7365	42.9	0.00097	0.125	698.65	134.93	924	75.61	14.60
M33	0.7365	42.9	0.00109	0.125	758.49	78.35	924	82.08	8.48
M34	0.7365	42.9	0.00085	0.250	722.49	144.40	924	78.28	15.64
M35	0.7365	42.9	0.00097	0.250	775.52	71.83	924	84.02	7.78
M36	0.7365	42.9	0.00109	0.250	691.60	95.96	924	78.19	15.63
M41	0.0443	397	0.00078	0.125	101.26	90.47	350	83.93	7.77
M42	0.0443	397	0.00089	0.125	43.37	48.99	350	74.85	10.38
M43	0.0443	397	0.00100	0.125	97.50	79.59	350	27.86	22.74
M44	0.0443	397	0.00078	0.250	159.63	26.41	350	45.61	7.55
M45	0.0443	397	0.00089	0.250	113.73	27.47	350	32.49	7.85
M46	0.0443	397	0.00100	0.250	83.05	31.43	350	23.73	8.98

In analyzing the data for 1/8 inch diameter copper, the percentage of base metal strength of the weld joint seemed too small compared with other materials. After checking with the in-process graph from the data acquisition system, the graph showed that welding time of this material was too long, suggesting an error in calculating the optimal weld condition. As a result, data associated with the small diameter were thrown out. In addition, it was noticed that the percentage of base metal strength for the ¼ inch copper was too small as well. As a result, the optimum conditions for copper were

revised and a second set of data were collected. These changes are reflected in Table 4.3. However, statistical analysis of the first data for ¼ inches diameter is shown in appendices J and K.

Table 4.3. Revised set of results for ¼ inch diameter electrode.

Code	% Gas (by Weight)	Thermal Conductivity (0-100C $Wm^{-1}K^{-1}$)	Welding Time (ms)	Diameter (Inches)	Mean Strength (MPa)	SD (Mpa)	Base Material Strength (Mpa)	% Mean (%)	% SD (%)
M14	0.0373	37.5	0.00085	0.250	649.52	15.56	715	90.84	2.18
M15	0.0373	37.5	0.00097	0.250	658.97	31.39	715	92.16	4.39
M16	0.0373	37.5	0.00109	0.250	625.33	25.44	715	87.46	3.56
M24	0.0033	397	0.00078	0.250	282.63	10.75	350	80.75	3.07
M25	0.0033	397	0.00089	0.250	254.79	21.42	350	72.80	6.12
M26	0.0033	397	0.00100	0.250	199.37	23.33	350	56.96	6.67
M34	0.7365	42.9	0.00085	0.250	722.49	144.40	924	78.19	15.63
M35	0.7365	42.9	0.00097	0.250	775.52	71.83	924	83.93	7.77
M36	0.7365	42.9	0.00109	0.250	691.60	95.96	924	74.85	10.38
M44	0.0443	397	0.00078	0.250	319.11	7.11	350	91.17	2.03
M45	0.0443	397	0.00089	0.250	227.65	42.25	350	65.04	12.07
M46	0.0443	397	0.00100	0.250	247.04	41.06	350	70.58	11.73

4.3.2 Confounding Variables

When the experiment was designed, it was intended to be orthogonal. Orthogonal design is a property that the estimator of all regression coefficients are uncorrelated which is Cov ($\beta i,\beta j$) = 0, where Cov ($\beta i,\beta j$) is the covariance of βi and βj which described how two variables covary. However, in running a designed experiment, it is sometimes difficult to reach and hold the precise factor levels required by the design. By considering the level of percentage of gas content in the base material, this experiment cannot hold precise factor level as shown in Table 4.4.

Table 4.4. Comparison between the designed percentage of gas content in base material level and actual percentage of gas content in base material level.

Material	Code for % Gas Level (Designed)	%Gas (By weight)	Code for % Gas (Actual)
Stainless Steel	-1	0.0373	-0.907
Low Oxygen Copper	-1	0.0033	-1
Nitronic 50 Steel	1	0.7365	1
Copper	1	0.0443	-0.888

As a result, it is impossible to identify the separate contributions of percentage of gas content in base material and thermal conductivity. Because of this confounding, there may be many models that can fit these data. However, according to the principle of

Occam's Razor, the simple models are to be preferred over the complicated ones; therefore, models that can explain the physical behavior of this data are preferred.

4.4 Analysis of Mean Weld Strength

The search for a suitable subset of independent variables may encompass a large array of possible models. Sequential variable selection procedures offer the option of exploring some of the possible models. After fitting all possible subset models, those that satisfy some model fitting criteria will be identified. The reason to apply strategic for variable selection is to exclude redundant and unnecessary variables, which yield less precise inference. The dependent variable in this analysis is the mean of CD weld strength as a percentage of base material strength (%Mean). The independent variables are thermal conductivity (Ther); percentage of gas content in the base material (Gas); welding time (Tw) and all interaction terms of main effects.

4.4.1 Forward Selection

The forward selection method begins with a constant mean as its current model and adds independent variables one at a time until no further addition significantly improves the fit. The following is the model from the forward selection method:

$$\% \text{ Mean} = 111912.06 - 344.81\text{Ther} - 0.028\ \text{TherXTw} + 2783.29\ \text{Gas}^2 + 0.79\ \text{Ther}^2 \quad (4.2)$$

where %Mean is the mean of CD weld strength as a percentage of base material strength; Ther is thermal conductivity; Tw is welding time; and Gas is the percentage of gas content in the base material.

Table 4.5.The estimates of the coefficient in the multiple regression of %Mean on thermal conductivity (Ther); percentage of gas content in base material (Gas); and welding time (Tw) (forward selection method).

Variable	Degree of Freedom	Estimate	Standard Error	T Statistic	P- Value
Intercept	1	11912.06	9980.42	1.1935	0.2715
Ther	1	-344.81	291.104	-1.1845	0.2749
TherXTw	1	-0.028	0.0071	-3.9611	0.0055
Gas^2	1	2783.29	2367.1	1.1758	0.2781
$Ther^2$	1	0.79	0.6699	1.1843	0.2749

Table 4.6. The analysis of variance for screening experiment data (forward selection method).

Source	Degree of Freedom	Sum of Squares	Mean Square	F Statistic	P Value
Model	4	1143.24	285.811	8.93	0.0070
Error	7	224.081	32.0116		
C total	11	1367.33			

From Table 4.5 and 4.6, there is evidence that the regression of the % Mean on thermal conductivity (Ther); the interaction term between welding time and thermal conductivity (Ther X Tw); the quadratic term of percentage of gas content in the base material (Gas^2); and the quadratic term of thermal conductivity ($Ther^2$) can explain 1149.24/1367.33 or 83.61% of the total variation in the observed distance. However, 16.39% of the variation in distances remains unexplained. The P-value of 0.007 in Table 4.6 is less than 0.01. As a result, there is a significant relation between the variables at a 99% confidence interval

4.4.2 Backward Elimination

The initial current model contains all possible independent variables, and then the redundant variables are removed one at a time until no further variable removal is possible. This is the model for the backward elimination method:

$$\% \text{ Mean} = 91.9762 - 20.1189\ Gas^2 - 0.0480\ Ther - 0.0281\ Ther\ X\ Tw \qquad (4.3)$$

where %Mean is the mean of CD weld strength as a percentage of base material strength; Ther is thermal conductivity; Tw is welding time; and Gas is percentage of gas content in the base material.

Table 4.7. The estimates of the coefficient in the multiple regression of %Mean on thermal conductivity (Ther); percentage of gas content in base material (Gas); and welding time (Tw) (backward elimination method).

Variable	Degree of Freedom	Estimate	Standard Error	T Statistic	P- Value
Intercept	1	91.9762	3.7144	24.7624	0.0001
Gas^2	1	-20.1189	8.6853	-2.3150	0.0492
Ther	1	-0.048	0.0114	-4.2093	0.0030
TherXTw	1	-0.281	0.0073	-3.8651	0.0048

Table 4.8. The analysis of variance for screening experiment data (backward elimination method).

Source	Degree of Freedom	Sum of Squares	Mean Square	F Statistic	P Value
Model	3	1098.34	366.115	10.89	0.0034
Error	8	268.982	33.6227		
C total	11	1367.33			

From Table 4.7 and 4.8, there is evidence that the regression of the %Mean on the quadratic term of percentage of gas content in the base material (Gas^2); thermal conductivity (Ther); and the interaction term between welding time and thermal conductivity (Ther X Tw) can explain 1098.34/1367.33 or 80.33% of the total variation in the observed distance. However, 19.67% of the variation in distances remains

unexplained. The P-value of 0.0034 in Table 4.8 is less than 0.01. As a result, there is a significant relationship between the variables at a 99% confidence interval.

4.4.3 Model Selection

Since both the forward selection and the backward elimination methods can be possible models, criteria should be used to select the model for this study. When comparing the models that have different numbers of parameters, R-squared leads to selecting the model with all variables. Considering R-squared of the models from both the forward selection and the backward elimination methods, although the 83.61% R-squared value of the forward selection model is better than the 80.33% R-squared value of the backward elimination model, the P-value of the coefficient of the independent variable in the backward elimination model is more significant than those in the forward selection model.

In determining which model is suitable, the P-value on the coefficient of the independent variable is the another criteria. The highest P-value in the independent variable from the forward selection model is 0.2781, which belongs to Gas^2. Since this P-value is greater than 0.10, that term is not statistically significant at the 90% confidence level. Also, the P-value of the coefficient for thermal conductivity and the quadratic term of thermal conductivity are 0.2749, which is not statistically significant at the 90% confidence level as well. On the other hand, the highest P-value in the coefficient of the independent variable from the backward elimination model is 0.0492, which belongs to Gas^2 as well. This term, therefore, is statistically significant at the 95% confidence level because this P-value is lower than 0.05.

Table 4.9. Comparison P-value of coefficient in multiple regression model from forward selection method and backward elimination method (percentage of mean data).

Forward Selection		Backward Elimination	
Variable	P-value	Variable	P-value
Intercept	0.2715	Intercept	0.0001
Ther	0.2749	Ther	0.0030
TherXTw	0.0055	TherXTw	0.0048
Gas^2	0.2781	Gas^2	0.0492
$Ther^2$	0.2749		

In addition, the P-value of the analysis of variance tables of both models is less than 0.01; there is statistically a relationship between the variables at the 99% confidence level. However, the P-value of 0.0034 from the analysis of variance table of the backward elimination model is lower than the P-value of 0.007 from the analysis of variance table of the forward selection model. As a result the model from the backward elimination method is more appropriate than that from the forward selection method.

4.4.4 Regression Model for Mean Weld Strength Data

Although the model from backward elimination is more appropriate, the quadratic term of percentage of gas content in the base material (Gas^2) seem not to associate with data since points in data of percentage of gas content in the base material trend to be a straight line. Moreover, the quadratic term of gas content in the base material is hard to

interpret in the data. According to the principle of Occam's Razor that the simple models are to be preferred over the complicated one, the percentage of gas content in the base material (Gas) was used to replace the quadratic term of percentage of gas content in base material (Gas^2). The following is the model after replacing Gas^2 by Gas:

$$\% \text{ Mean} = 92.3495 - 15.0918 \text{ Gas} - 0.0481 \text{ Ther} - 0.0281 \text{ Ther X Tw} \quad (4.4)$$

where %Mean is the mean of CD weld strength as a percentage of base material strength; Ther is thermal conductivity; Tw is welding time; and Gas is the percentage of gas content in the base material.

Table 4.10.The estimates of the coefficient in the multiple regression of %Mean on thermal conductivity (Ther); percentage of gas content in base material (Gas); and welding time (Tw) (selected model).

Variable	Degree of Freedom	Estimate	Standard Error	T Statistic	P- Value
Intercept	1	92.3495	3.9616	23.3113	0.0001
Gas	1	-15.0918	6.8335	-2.20851	0.0582
Ther	1	-0.0481	0.0118	-4.9016	0.0035
TherXTw	1	-0.0281	0.0074	-3.7939	0.0053

Table 4.11. The analysis of variance for screening experiment data (selected model).

Source	Degree of Freedom	Sum of Squares	Mean Square	F Statistic	P Value
Model	3	1088.14	362.715	10.39	0.0039
Error	8	279.182	34.8978		
C total	11	1367.33			

From Table 4.10, both the P-value of 0.0035 for the coefficient of thermal conductivity (Ther) and the P-value of 0.0053 for the coefficient of interaction term between thermal conductivity and welding time (TherXTw) are less than 0.01. As a result, those values indicate the strong evidence that thermal conductivity (Ther) and interaction term between thermal conductivity and welding time (TherXTw) are associated with the percentage of the CD weld strength mean with base material strength (%Mean) at a 99% confidence level. However, the P-value for the coefficient of percentage of gas content in base material (Gas) is 0.0582. Although this value doesn't indicate convincing evidence, it is suggestive (but inclusive) that the percentage of gas the content in base material associates with percentage of CD weld strength mean with base material strength (%Mean) at a 94% confidence level.

In addition, the P-value of 0.0039 from Table 4.10 shows that there is evidence that the percentage of the CD weld strength mean with base material strength (% Mean) associates with thermal conductivity (Ther); percent of gas content in material (Gas); and the interaction term between thermal conductivity and welding time (Ther X Tw). Also,

R-squared indicates that there is evidence that the regression of the %Mean on the percentage of gas content in the base material (Gas); thermal conductivity (Ther); and the interaction term between welding time and thermal conductivity (Ther X Tw) can explain 1088.14/1367.33 or 79.58% of the total variation in the observed distance. However, 21.42% of the variation in distances remains unexplained.

4.4.5 Validating Models

Table 4.12 shows the result of validating data of three models: the forward selection model, the backward elimination model and the selected model. It is noticed that the predicted value and a 95% confidence interval of the backward elimination model and selected model are almost the same. On the other hand, the predicted value from the forward selection model is obviously different from the experimental value, and a 95% confidence interval from forward selection model is too broad. Experimental value for magnesium is not associated with predicted value for any models. Also, experimental value of magnesium is not within 95% confidence interval of any model while the experimental value of mild steel is. As a result, the experimental %Mean value is not consistent with the regression model. There may be other sources that can affect the mean strength of a CD weld joint such as oxide. In magnesium, magnesium oxide is brittle and easy to form. Consequently, with magnesium oxide between a CD weld joint, CD weld joint strength trends to be lower than usual.

Table 4.12. Validating model for mean weld strength data.

Model	Material	Experimental %Mean Value	Predicted %Mean Value	% Error	95% Confidence Interval
Forward Selection Model	Magnesium	65.73	-22516.4	34355.3	-67650-22617
	Mild Steel	97.14	5963.3	6038.9	-5760.1-17686
Backward Elimination Model	Magnesium	65.73	88.87	35.20	74.18 – 103.6
	Mild Steel	97.14	91.61	5.69	75.92 – 107.3
Selected Model	Magnesium	65.73	89.05	35.47	74.01-104.1
	Mild Steel	97.14	91.85	5.44	75.73-108.0

4.5 Analysis of Weld Strength Variability

The dependent variable in this analysis is the percentage of CD weld strength standard deviation with base material strength (%SD). The independent variables are thermal conductivity (Ther); percentage of gas content in the base material (Gas); welding time (Tw); and all interaction terms of main effects. Like the analysis of mean strength, a strategy for variable selection was applied to select a model that can interpret data.

However, the scatterplots (appendix L) of the dependent variable versus the independent variable reveal that dependent variable needs to be transformed. A natural log (ln) transformation was applied to independent variable (%SD).

4.5.1 Forward Selection

The following is the model from the forward selection method:

$$\ln(\%SD) = -4.0302 + 0.1566Ther + 0.0170TherXGas - 0.3408GasXTw + 0.0016TherXTw - 0.0036\,Ther^2 - 0.2923Tw^2 \quad (4.5)$$

where ln(%SD) is the natural log of the standard deviation of CD weld strength as a percentage of base material strength; Ther is thermal conductivity; Tw is welding time; and Gas is the percentage of gas content in the base material.

Table 4.13.The estimates of the coefficient in the multiple regression of ln(%SD) on thermal conductivity (Ther); percentage of gas content in base material (Gas); and welding time (Tw) (forward selection method).

Variable	Degree of Freedom	Estimate	Standard Error	T Statistic	P- Value
Intercept	1	-4.0302	6.1072	-0.6598	0.5386
Ther	1	0.1567	0.1760	0.8898	0.4143
TherXGas	1	0.1701	0.0226	0.7535	0.4851
GasXTw	1	-0.3408	0.4343	-0.7847	0.4682
TherXTw	1	0.0016	0.00057	2.8720	0.0349
$Ther^2$	1	-0.0036	0.00040	-0.8863	0.4160
Tw^2	1	-0.2923	0.2757	-1.0604	0.3375

Table 4.14. The analysis of variance for screening experiment data (forward selection method).

Source	Degree of freedom	Sum of Squares	Mean Square	F Statistic	P Value
Model	6	4.2312	0.7053	3.48	0.0962
Error	5	1.0133	0.2027		
C total	11	5.2445			

From Table 4.13 and 4.14, there is evidence that the regression of ln(%SD) on thermal conductivity (Ther); the interaction term between thermal conductivity and percentage of gas content in the base material (Ther X Gas); the interaction term between percentage of gas content in base material and welding time (Gas X Tw); the interaction term between thermal conductivity and welding time (Ther X Tw); quadratic term of thermal conductivity ($Ther^2$); and the quadratic term of the percentage of gas content in the base material (Gas^2) can explain 4.2312/5.2445 or 80.68% of the total variation in the observed distance. However, 19.32% of the variation in distances remains unexplained. The P-value of 0.0962 in Table 4.14 is less than 0.1. As a result, there is a relationship between the variables at a 90% confidence interval.

4.5.2 Backward Elimination

The following is the model from the backward elimination method:

$$\% \text{ SD} = 1.0992 + 1.7377\text{Gas} + 0.00000386\text{Ther}^2 + 0.0016 \text{ TherXTw} \quad (4.6)$$

where ln(%SD) is the natural log of the standard deviation of CD weld strength as a percentage of base material strength; Ther is thermal conductivity; Tw is welding time; and Gas is the percentage of gas content in the base material.

From Table 4.15 and 4.16, there is evidence that the regression of ln(%SD) on the percentage of gas content in the base material (Gas); the quadratic term of thermal conductivity (Ther^2); and the interaction term between welding time and thermal conductivity (Ther X Tw) can explain 3.8148/5.2445% or 72.74% of the total variation in the observed distance. However, 27.26% of the variation in distances remains unexplained. the P-value of 0.012 in table 4.16 is less than 0.02. As a result, there is a significant relationship between the variables at a 98% confidence interval.

Table 4.15. The estimates of the coefficient in the multiple regression of the ln(%SD) on thermal conductivity (Ther); percentage of gas content in base material (Gas); and welding time (Tw) (backward elimination method).

Variable	Degree of Freedom	Estimate	Standard Error	T Statistic	P- Value
Intercept	1	1.0992	0.2594	4.2377	0.0028
Gas	1	1.7377	0.4921	3.5311	0.0077
Ther^2	1	3.68 E –6	1.94 E –6	1.9920	0.0815
TherXTw	1	0.0016	0.00053	2.9775	0.0177

Table 4.16. The analysis of variance for screening experiment data (backward elimination method).

Source	Degree of Freedom	Sum of Squares	Mean Square	F Statistic	P Value
Model	3	3.8148	1.2716	7.12	0.0120
Error	8	1.4297	0.1787		
C total	11	5.2445			

4.5.3 Model Selection

Since both the forward selection and the backward elimination methods can be possible model, criteria should be use to select the model for this study. When comparing the models that have different numbers of parameters, R-squared leads to selecting the model with all variables. Considering R-squared of models from both the forward selection and the backward elimination methods, although the 80.68% R-squared value of the forward selection model is higher than the 72.74% R-squared value of the backward elimination model, the P-value of coefficient of independent variables in the backward elimination model is more significant than those in the forward selection model.

Table 4.17. Comparison of P-value of coefficient in multiple regression model from forward selection method and backward elimination method (CD weld strength standard deviation data).

Forward Selection		Backward Elimination	
Variable	P-value	Variable	P-value
Intercept	0.5386	Intercept	0.0028
Ther	0.4143	Gas	0.0077
TherXGas	0.4851	$Ther^2$	0.0815
GasXTw	0.4682	TherXTw	0.0177
TherXTw	0.0349		
$Ther^2$	0.4160		
Tw^2	0.3375		

In determining which model is suitable, the P-value of the coefficient of the independent variable is the another criteria. The highest P-value in the independent variable from the forward selection model is 0.4851, which belongs to TherXGas. Since this P-value is greater than 0.10, that term is not statistically significant at the 90% confidence level. Also, the P-value of the coefficient for thermal conductivity (Ther); the interaction term of thermal conductivity and the percentage of gas content in the base material (TherXGas); the interaction term of the percentage of gas in the base material and welding time (GasXTw); the quadratic term of thermal conductivity ($Ther^2$), and the quadratic term of welding time (Tw^2) are 0.4143, 0.4851, 0.4682, 0.4146, and 0.3375 respectively, which are not statistically significant at a 90% confidence level as well. On

the other hand, the highest P-value in the coefficient of the independent variable from the backward elimination model is 0.0815, which belongs to $Ther^2$. Although this term is not convincing it is suggestive (but inconclusive) at a 90% confidence level because this P-value is lower than 0.1.

In addition, the P-value of 0.012 of the analysis of variance tables of the backward elimination model is less than 0.02; thus, there is statistically relationship between the variables at the 98% confidence level. On the other hand, the P-value of 0.0962 from the analysis of variance table of the forward selection model is lower than 0.1; there is a statistically significant relationship between the variables at a 90% confidence level which is lower than that of the backward selection model. As a result, the backward elimination model is more appropriate than that of forward selection.

4.5.4 Regression Model for Weld Strength Variability Data

Like the regression model for mean weld strength data, the quadratic term of thermal conductivity ($Ther^2$) from the backward elimination model seems not to associate to the data since points in data of thermal conductivity trends to be a straight line. Moreover, the quadratic term of thermal conductivity is hard to interpret by the data. According to the principle of Occam's Razor that the simple models are to be preferred over the complicated one, thermal conductivity (Ther) was used to replace the quadratic term of thermal conductivity ($Ther^2$). The following is the model after replacing $Ther^2$ by Ther:

$$\ln(\%\ SD) = 1.0422 + 1.7272Gas + 0.0017Ther + 0.0016TherXTw \qquad (4.7)$$

where ln(%SD) is the natural log of the standard deviation of CD weld strength as a percentage of base material strength; Ther is thermal conductivity; Tw is welding time; and Gas is the percentage of gas content in the base material.

Table 4.18. The estimates of the coefficient in the multiple regression of ln(%SD)on thermal conductivity (Ther); percentage of gas content in base material (Gas); and welding time (Tw) (selected model).

Variable	Degree of Freedom	Estimate	Standard Error	T Statistic	P- Value
Intercept	1	1.0422	0.2835	3.6759	0.0063
Gas	1	1.7272	0.4891	3.5314	0.0077
Ther	1	0.0017	0.0008	1.9914	0.0816
TherXTw	1	0.0016	0.0005	2.9772	0.0177

Table 4.19. The analysis of variance for screening experiment data (selected model).

Source	Degree of freedom	Sum of Squares	Mean Square	F Statistic	P Value
Model	3	3.8146	1.2715	7.11	0.0120
Error	8	1.4299	0.1787		
C total	11	5.2445			

From Table 4.18, both p-value of 0.0077 for the coefficient of percentage gas content in the base material (Gas) and the P-value of 0.0177 for the coefficient of interaction term between thermal conductivity and welding time (TherXTw) are less than 0.02. As a result, those values indicate the strong evidence that the percentage of gas content in the base material (Gas) and the interaction term between thermal conductivity and welding time (TherXTw) associate with ln(%SD) at a 98% confidence level. However, the P-value of 0.0817 for the coefficient of percentage of thermal conductivity (Ther) is less than 0.085. Although this value doesn't indicate convincing evidence, it is suggestive (but inclusive) that thermal conductivity associates with ln(%SD) at a 91.5% confidence level.

In addition, the P-value of 0.012 from Table 4.19 shows that there is evidence that ln(%SD) associates with thermal conductivity (Ther); percent of gas content in material (Gas); and the interaction term between thermal conductivity and welding time (TherXTw) at a 98% confidence level. Also, R-squared indicates that there is evidence that the regression of ln(%SD) on the percentage of gas content in material (Gas); thermal conductivity (Ther); and the interaction term between welding time and thermal conductivity (Ther X Tw) can explain 3.8146/5.2445 or 72.74% of the total variation in the observed distance. However, 27.26% of the variation in distances remains unexplained.

4.5.5 Validating Models

The table below presents the validating model for weld strength variability data. It is noticed that a % error and a 95 % confidence interval of the selected model and the backward elimination model are almost the same while from the forward selection, the predicted values of both materials are too high and the 95% confidence intervals of both materials are too broad. In addition, the experimental value of magnesium and mild steel are in a 95% confidence interval for both the selected model and the backward elimination model. From validating the selected model, although the predicted % SD value of both magnesium and mild steel are not associated with the experimental % SD value, predicted values are between a 95% confidence interval. Consequently, the experimental value is not inconsistent with the regression model.

Table 4.20. Validating model for weld CD weld strength standard deviation data.

Model	Material	Experimental %SD Value	Predicted %SD Value	% Error	95% Confidence Interval
Forward Selection Model	Magnesium	6.49	70969.1	1.09E4	9.5E7 – 1.3E18
	Mild Steel	5.67	0.19	96.65	6.57E-5 – 572.5
Backward Elimination Model	Magnesium	6.49	2.64	59.32	0.86 – 8.00
	Mild Steel	5.37	2.97	44.69	0.95 – 9.68
Selected Model	Magnesium	6.49	2.94	54.70	1.00 – 8.58
	Mild Steel	5.37	2.89	46.18	0.91 – 8.41

4.6 Fracture Surfaces and Weld Area

From the fracture surface picture (Figure 4.1- 4.8), we can see the following:

1. In comparison between Nitronic 50 steel and stainless steel, the pictures show voids present in both materials. However, the void in the Nitronic 50's fracture surface is more than that of the stainless steel due to the higher amount of gas in Nitronic 50. Also, this void causes a lower weld area in Nitronic 50's fracture surface.
2. In comparison between low oxygen copper and first set of plain copper, there is a greater number of voids in plain copper, indicating the more gas present the greater the number of the void.
3. There is presolidification present on both low oxygen copper's and copper's fracture surfaces. In a high thermal conductivity material, presolidification has a greater propensity to happen.
4. In low oxygen copper and plain copper, presolidification seems to be present more when the welding time is increased. As a result, the welding time has some effect on the variability in a weld joint.

Beside the destructive tensile test, the specimens were examined by using a thermal printer to estimate the weld area of each material. One sample of each material was chosen.

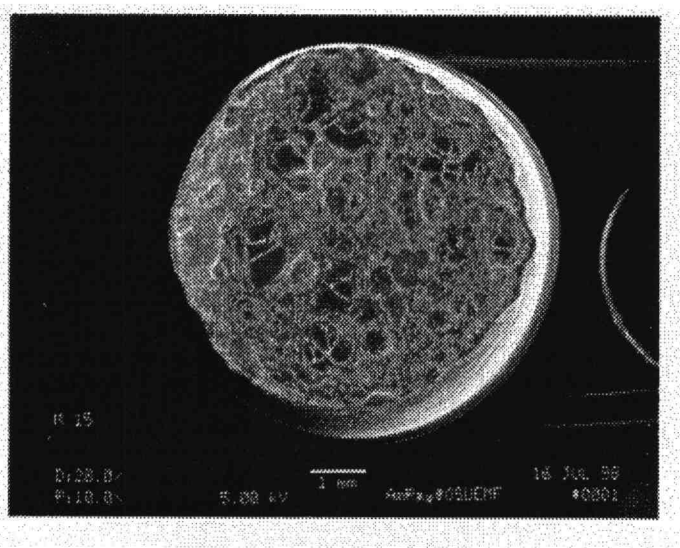

Figure 4.1. Fracture surface of stainless steel at Tw = 0.

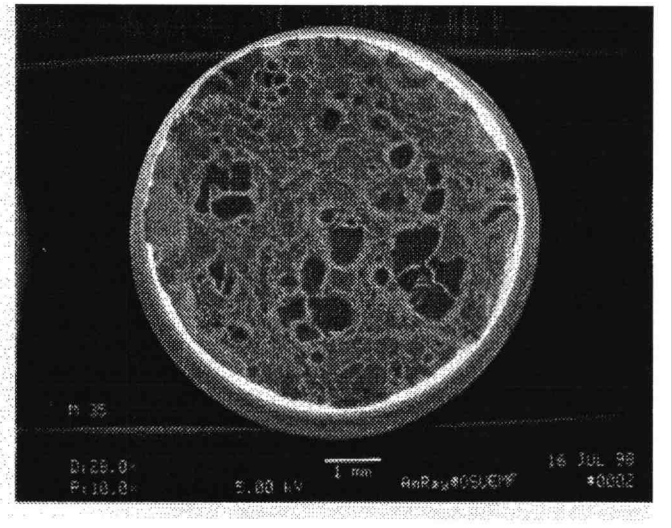

Figure 4.2. Fracture surface of Nitronic 50 steel at Tw = 0.

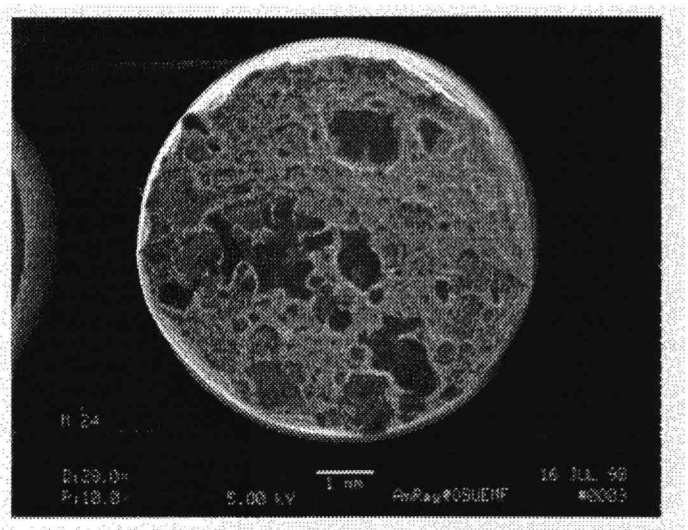

Figure 4.3. Fracture surface of low oxygen copper at Tw = -1.

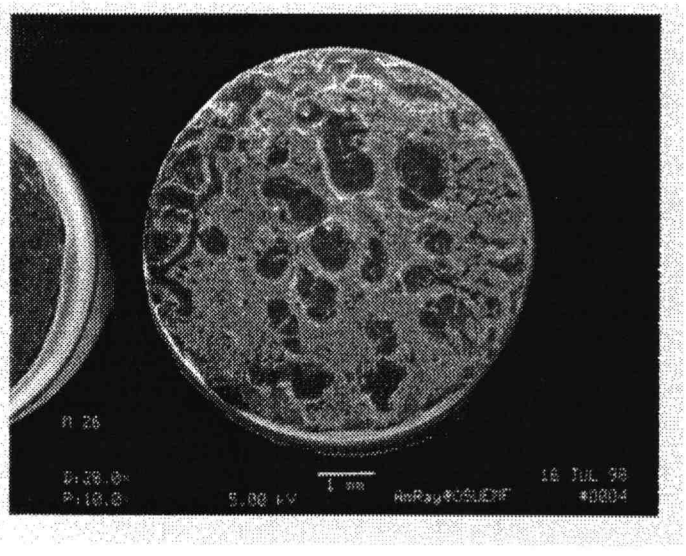

Figure 4.4. Fracture surface of low oxygen copper at Tw = 1.

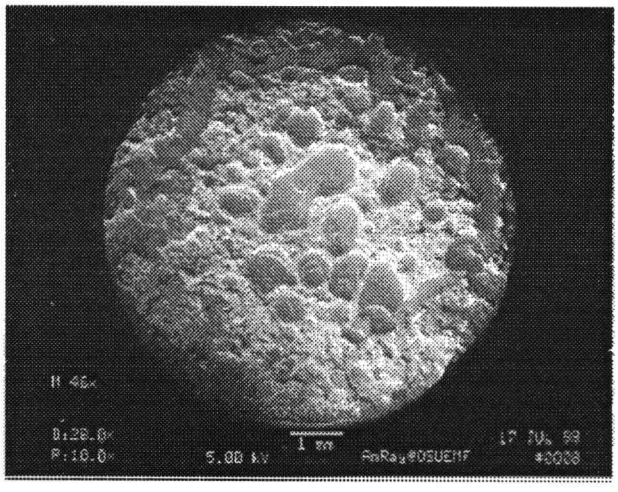

Figure 4.5. Fracture surface of copper at Tw = -1 (first data).

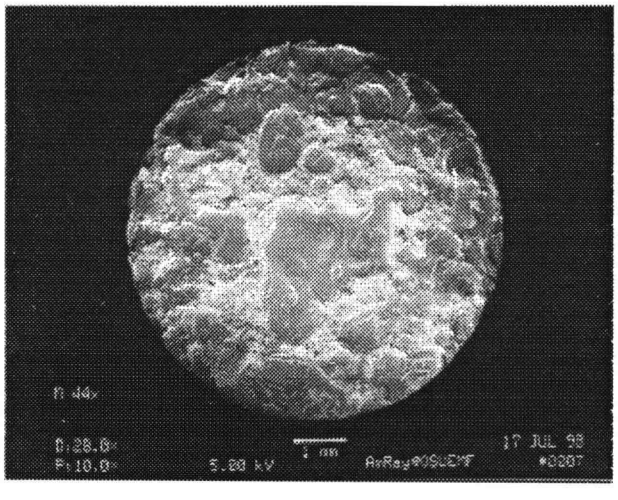

Figure 4.6. Fracture surface of copper at Tw = -1 (first data).

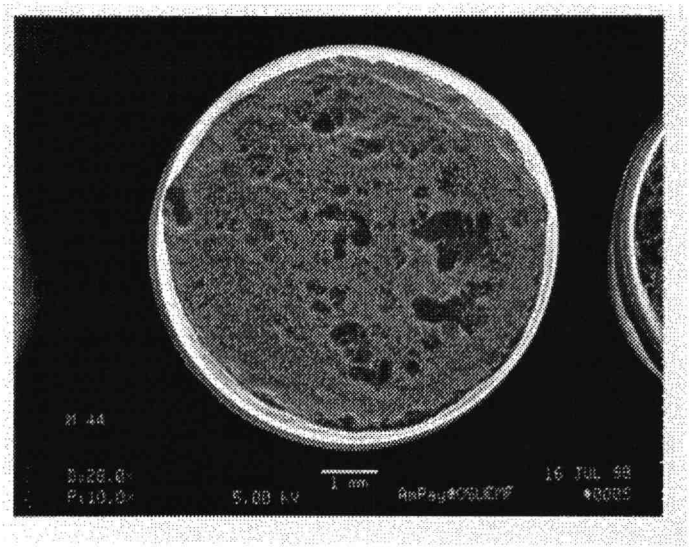

Figure 4.7. Fracture surface of copper at Tw = -1 (revised data).

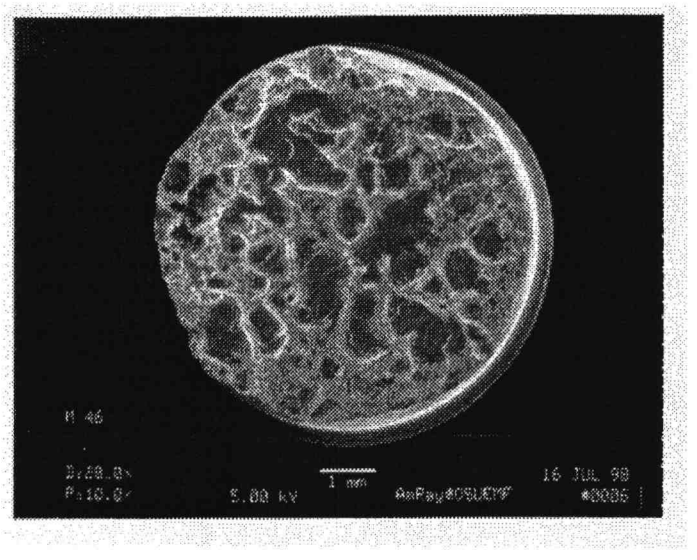

Figure 4.8. Fracture surface of copper at Tw = 1 (revised data).

Table 4.21. Percentage of estimated weld area of each material.

Materials	Code	% CD Strength	Percentage of Weld Area
Stainless Steel	M 14	90.87	85.26
	M15	93.37	83.40
	M16	91.19	84.30
Low Oxygen Copper	M24	78.05	82.10
	M25	75.53	78.98
	M26	61.67	58.00
Nitronic 50 steel	M34	81.60	83.05
	M35	75.12	83.03
	M36	74.53	79.60
Copper	M44	89.73	86.67
	M45	77.41	78.11
	M46	60.37	55.18

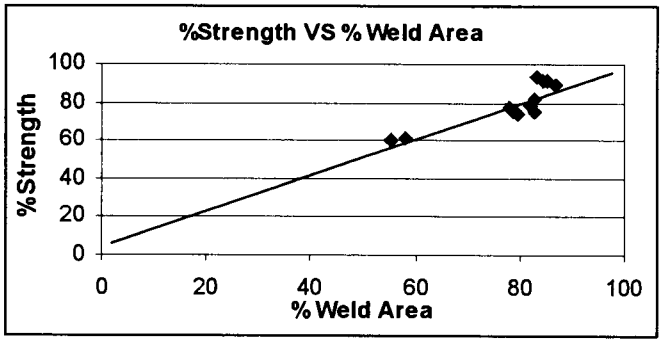

Figure 4.9. Graph between percentage of CD weld strength with base material strength and percentage of estimated weld area.

The graph in Figure 4.9 shows that all observed points tend to be a straight line. This suggests that weld strength and variability are mainly affected by voids.

4.7 Discussion

1. From the regression model of the mean strength as a percentage of base material strength:

$$\% \text{ Mean} = 92.3495 - 15.0918 \text{ Gas} - 0.0481 \text{ Ther} - 0.0281 \text{ Ther X Tw} \quad (4.9)$$

where %Mean is the mean of CD weld strength mean as a percentage of base material strength; Ther is thermal conductivity; Tw is welding time; and Gas is the percentage of gas content in the base material. The interaction term of conductivity and welding time expresses the regression of %Mean on thermal conductivity for different levels of welding time as follows:

$$\% \text{ Mean} = 92.3495 - 15.0918 \text{ Gas} - 0.0200\text{Ther} \quad (4.10)$$

$$\% \text{ Mean} = 92.3495 - 15.0918 \text{ Gas} - 0.0481\text{Ther} \quad (4.11)$$

$$\% \text{ Mean} = 92.3495 - 15.0918 \text{ Gas} - 0.0762\text{Ther} \quad (4.12)$$

The coefficient of thermal conductivity was changed from global slope, -0.0281 to -0200, -0.0762 at –1 Tw level and 1 Tw level respectively. However, the coefficient of thermal conductivity was not changed at 0 Tw level. We can observe that the absolute value of the coefficient of thermal conductivity of the 1 Tw level is the highest and that of –1 Tw level is the lowest. To isolate the thermal conductivity and welding time terms, copper and stainless steel data may be compared since the percentages of gas content are similar. From above three regression models and Figure 4.10 reveal that thermal conductivity much more affects the %Mean when the welding time is increased.

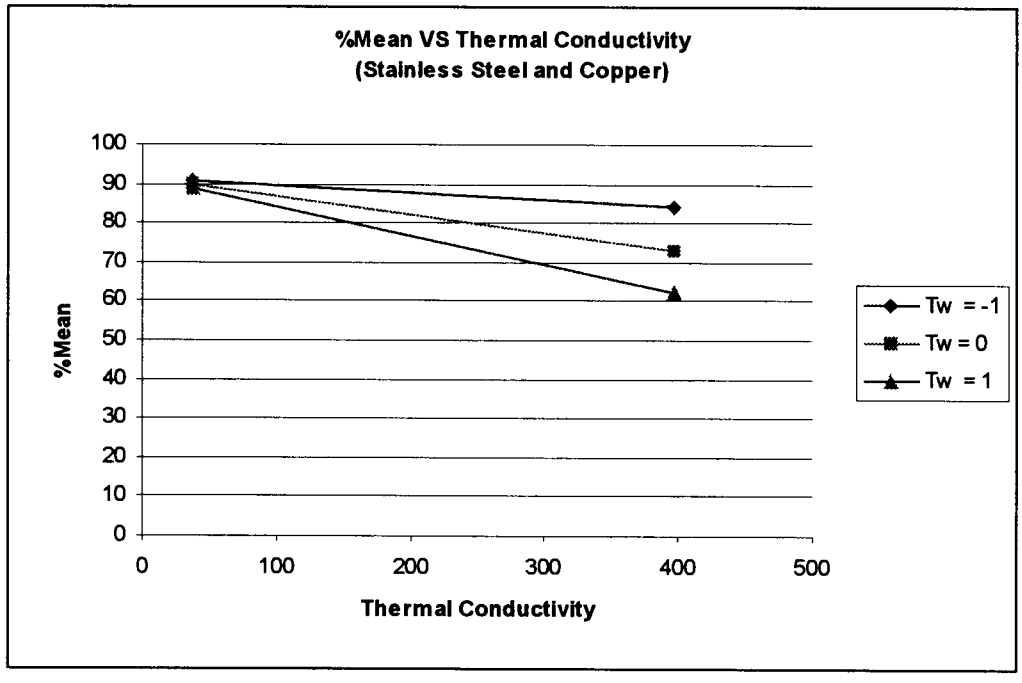

Figure 4.10. Graph %Mean and thermal conductivity.

Also, considering the regression model of standard deviation of the weld strength as a percentage of base material strength:

$$\ln(\%SD) = 1.0422 + 1.7272Gas + 0.0017Ther + 0.0016TherXTw \quad (4.13)$$

where ln(%SD) is the natural log of the standard deviation of CD weld strength as a percentage of base material strength; Ther is thermal conductivity; Tw is welding time; and Gas is the percentage of gas content in the base material. The interaction term of conductivity and welding time expresses the regression of ln(%SD) on thermal conductivity for different levels of welding time as follows:

$$\ln(\%\ SD) = 1.0422 + 1.7272Gas + 0.0001Ther \quad (4.14)$$

$$\ln(\%\ SD) = 1.0422 + 1.7272Gas + 0.0017Ther \quad (4.15)$$

$$\ln(\%\ SD) = 1.0422 + 1.7272Gas + 0.0033Ther \quad (4.16)$$

Like the %Mean regression model, copper and stainless data were compared (Figure 4.11). These reveal that thermal conductivity much more affects ln(%SD) when the welding time is increased.

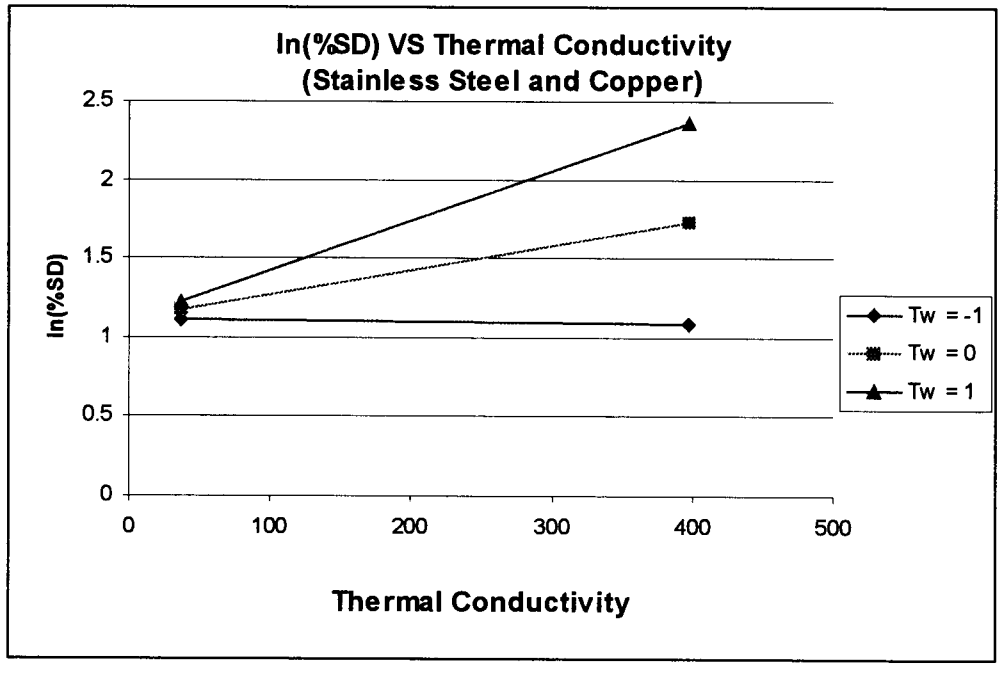

Figure 4.11. Graph ln(%SD) and thermal conductivity.

This suggests that the thermally conductive material is much more sensitive to welding time in comparison with the thermally insulative material. Figure 4.12 illustrates this point. At 80% strength of the base material, the welding time interval of the thermally insulative material yields a broader optimum RC/Tw ratio interval than that of the thermally conductive material. In addition, at the same percent change of RC/Tw ratio of both thermally conductive and thermally insulative materials, the percent change of

strength of the thermally conductive material is larger than that of the thermally insulative material.

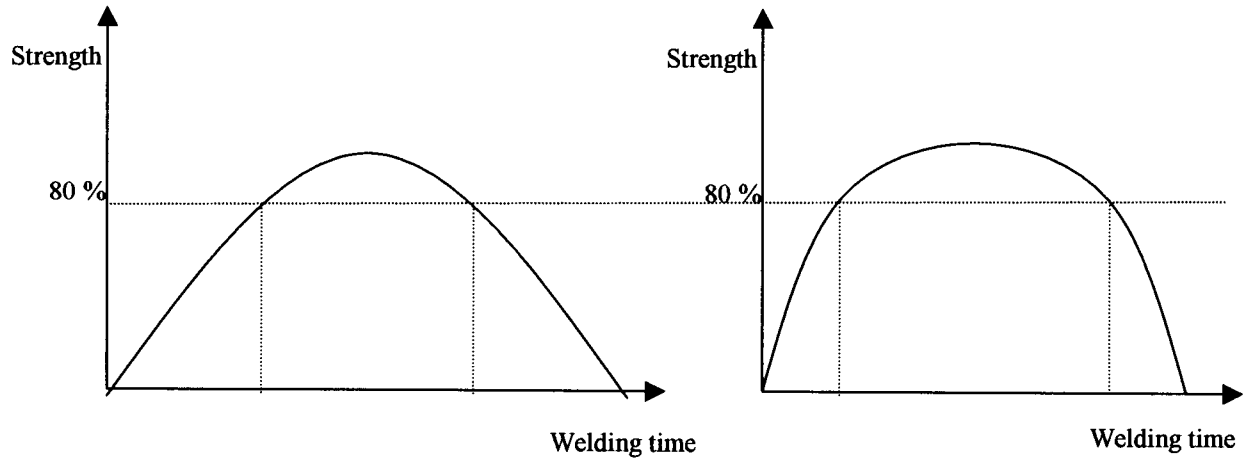

Figure 4.12. Comparison between thermally conductive and thermally insulative material.

The convincing evidences from the Scanning Electron Microscope (SEM) picture and statistical analysis show that thermal conductivity, percentage of gas content in the base material, and the interaction term between thermal conductivity and welding time significantly affect the CD weld strength mean and variability. Although the percentage of gas content in the base material is one of the sources of CD weld strength variability, automation technique cannot be taken to reduce the impact of outgassing. Automation techniques, however, can be applied to CDW system to reduce the impact of thermal conductivity to COV. The shorter the welding time, the less variability in CD weld strength. With an exactly known tip length and velocity at the minimum welding time,

the variability in CD weld strength can be decreased by automating the welding head velocity at impact.

The results of this experiment are limited due to the difficulty in establishing optimization conditions. If the condition for CD welding is far from optimum, the more variability seems to be present. This can introduce error into the data.

Oxide may be another potential source of variability in CD weld strength. In some materials in which oxides easily form, such as aluminum or magnesium, the CD weld strength seems to be lower than usual because aluminum oxide or magnesium oxide is brittle. As a result, the surface of both electrodes must be cleaned before welding. In addition, variability can be influenced by arc mode. So, using an arc stabilizer may reduce the variability in CD weld strength because the arc stabilizer can control arc in cold cathode materials such as copper and aluminum by preventing arc movement which makes the electrode temperature even.

It is noticed that the standard deviation of Nitronic 50 at welding time level = -1 (M34) is pretty high in comparison with other standard deviation of other codes. However, the residual plots between residual and predicted value (Appendices D and E) show that data from code M34 is not outlier. As a result, this may be caused by gas in base material. Figures 4.13-4.16 contain SEM photomicrographs of fracture surface fore code M34. From the raw data in the appendix A, run No. 40 is shown to be the cause of high variability. Notice in run No. 40 that the gas seems to be spreading out from the center. This could indicate that for a short welding time, the gas has insufficient time to evolve and escape the weld zone before solidification. Notice the notch defect that is formed, accounting for the low weld strength. Weld strength variability in this set of data

is accounted for because gas bubble nucleation is a random phenomenon dependent upon thermal and gas solubility gradients in the material at the time of welding. It is suggested that the bevel angle of faying surfaces may have an impact on how fast gas is moved out of the fusion zone. Therefore, larger bevel angles may reduce weld strength variability in high gas content materials.

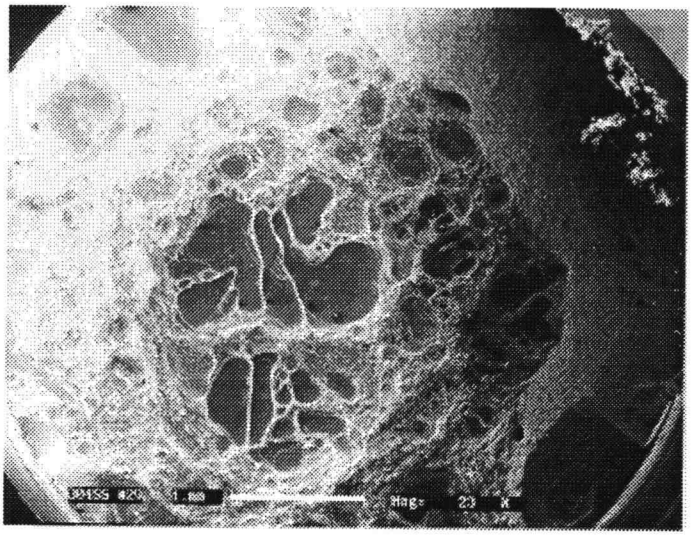

Figure 4.13. Fracture surface of Nitronic 50 steel CodeM34 run No.29

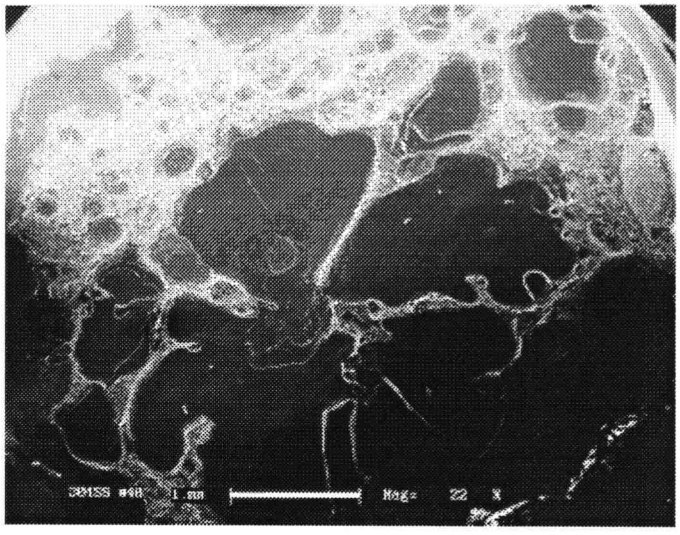

Figure 4.14. Fracture surface of Nitronic 50 steel CodeM34 run No.40

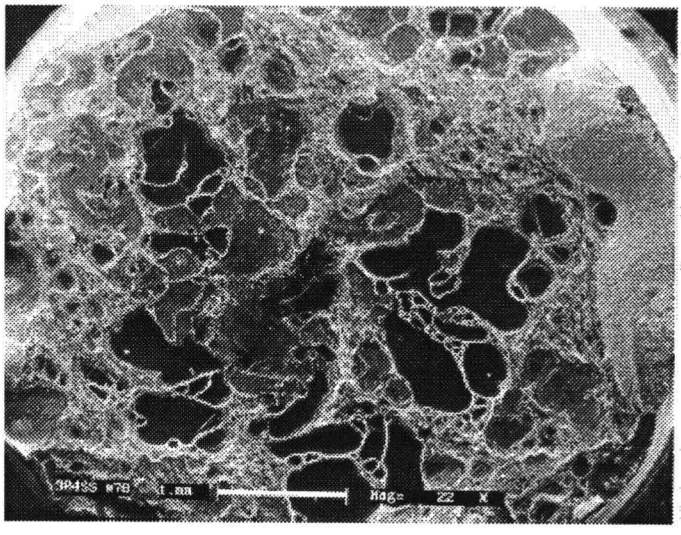

Figure 4.15. Fracture surface of Nitronic 50 steel CodeM34 run No.70

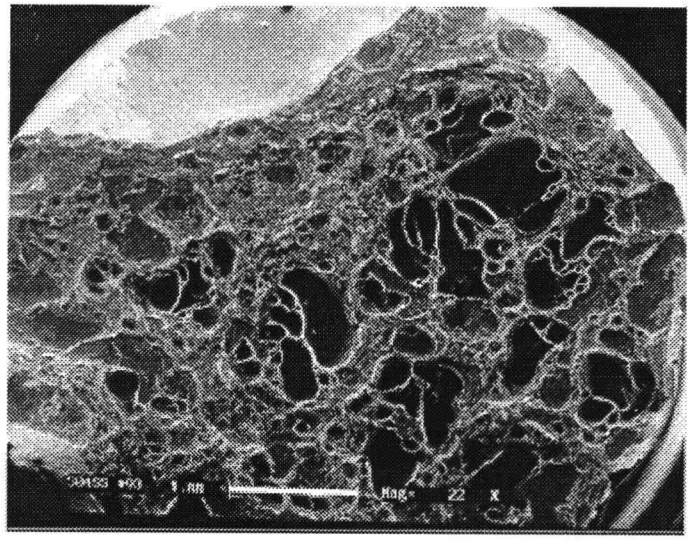

Figure 4.16. Fracture surface of Nitronic 50 steel CodeM34 run No.90

5. Conclusions

5.1 Conclusions

The objective of this study was to investigate the sources of weld strength variability in the initial gap method of the CDW process. Results show that the percent of gas content in the material affects weld strength variability in CDW at a 99% confidence level. In addition, thermal conductivity is shown to have a greater effect on variability as welding time is increased at a 98% confidence level. Thermal conductivity alone was found to affect variability at a 91% confidence level. The source of variability in CDW, therefore, is material-dependent.

Furthermore, the percentage of gas content in the base material affects to mean weld strength in CDW at a 94% confidence level, while thermal conductivity alone was found to affect the mean at a 99% confidence level. Like thermal conductivity, thermal conductivity is revealed to have a greater effect on the mean as welding time increase at a 99% confidence level.

With a high percentage of gas content in the base material, there is a high possibility that variability is present. Increasing the bevel angle may be a method for reducing variability. In addition, low welding time and automation to control impact velocity should be applied to the high thermal conductivity material for reducing variability. Moreover, the impact of thermal conductivity on CD weld strength variability is more predictable than that of the percentage of gas content in the base material.

Finally, it is impossible to identify the separate contributions of the percentage of gas content in the base material and thermal conductivity because these two independent

variables are confounding. There may be many models that can fit these data. However, the simple models are to be preferred over the complicated ones so the selected models for %Mean and ln(%SD) data are appropriate to interpret the data.

5.2 Future Research

The understanding of source of variability in the CDW process can be advantageous for guiding automation in CDW. According to this study, high thermal conductivity and the high percentage of gas content materials probably need to be automated because automation can lead to more consistency in the process. According to this study, there may be other variables that can affect CD weld strength variability and CD weld mean strength. Bevel angle may affect the size of voids. In addition, oxide and arc mode are also suspected to be sources of variability. Consequently, further investigation of other sources of variability in CD weld strength should be taken to understand more about CD weld strength variability.

BIBLIOGRAPHY

American Welding Society (AWS). 1991. Welding Handbook, vol. 2.

Baeslack III, W.A., K.H. Hou, and J.H. Devletian. 1989. Electron microscopy of rapidly solidified weldments in a powder metallurgy Al-Fe-Ce alloy. Journal of Materials Science letter 7 pp. 716-720.

Baeslack III, W.A., K.H. Hou, and J.H. Delvetian. 1988. Rapid solidification joining of a powder metallurgy Al-Fe-Ce alloy. Journal of Materials Science letter 7 pp.944-948.

Cary, H.B.1979. Modern Welding Technology, Prentice-Hall.

Cho, H.S., and D.W. Chun. 1985. A microprocessor-based electronic movement controller for spot welding quality assurance. IEEE Transactions on Industrial Electronics, vol. IE-32. N0.3.

Devletian, J.H. 1987. SiC/Al metal matrix composite welding by a capacitor discharge process. Welding Journal, vol. 66, no. 6, pp.33-39.

Faitel, W. 1995. Intelligent resistance welding. US Department of Commerce, National Institute of Standards and Technology submitted to the Advanced Technology Program Competition by the Intelligent Resistance Welding Consortium.

Fukushima, S., and T. Kasugai. 1990. Capacitor spot welding of Fe-Si-B amorphous alloy foil. Transaction of National Research Institute for Metals, vol. 32, no. 3, pp.81-90.

Giachino, J.W., W. Weeks, and G.S. Johnson. 1968. Welding Technology. American Technical Society.

Johnson, K.I. 1977. Voltage spot weld correction unit developed by the welding institute Resistance Welding Control and Monitoring, pp.19-28.

Klimpel, A. 1989. Investigation and quality control of resistance spot welding. Welding International, vol.3, no. 12, pp.1040-1045.

Lancaster, J.F., Metallurgy of Welding, Chapman & Hall, 1987.

Lanstorm, H. 1937. "Automatic resistance welding" Welding Journal.

Morgan-Warren, E.I. 1974. The control of arc stud welding. Advance in Welding Processes: Third International Conference, vol. 1, pp.1-7.

Norrish, J. 1992. Advanced Welding Processes. Institute of Physics Publishing.

Quihlan, A.L. 1955. Automatic percussion welding of telephone relay contacts. Welding Journal, pp. 237-240.

Ramirez, J.E. B. Han, and S. Liu. 1994. Effect of welding variables and solidification substructure on weld metal porosity. Metallurgical and Material Transaction, vol. 25a, pp.2285-2294.

Simmon, J.W., and R.D. Wilson. 1996. Joining of high-nitrogen stainless steel by capacitor discharge welding. Welding Research Supplement. vol. 75, no. 6, pp.185s-190s.

Venkataraman S., and J.H. Devletian. 1988. Rapid solidification of stainless steels by capacitor discharge welding. Welding Journal research supplement, vol. 67, no. 6, pp.111s-118s.

Wilson, R.D. 1991. A capacitor discharge weld microstructure model for iron aluminide. Ph.D. Dissertation, Oregon Graduate Institute, Oregon.

Wilson, R.D. 1996. Rapid solidification joining of silver electrical contacts to copper conductors using the capacitor discharge welding process. 11 th annual North American Welding research conference: Advance in welding technology, pp.203-211.

Wilson, R.D., D.E. Alman, and J.A. Hawk. 1995. Rapid solidification joining of intermatallics using capacitor discharge welding. Material Research Society Symposium Proceeding, vol. 364, pp.237-242.

Wilson, R.D., and J.A. Hawk. 1994. Rapid solidification joining using the capacitor discharge welding process. Metallurgical Processes for Early Twenty-First Century, pp.267-282.

Wilson, R.D., J.A. Hawk, and J.H. Devletian. 1993. Capacitor discharge weld modeling using ultra high speed photography. Materials Research Society Symposium Proceeding, vol. 314, pp.151-162.

Wilson, R.D., J.R. Woodyard, and J.H. Devletian. 1993. Capacitor discharge welding: Analysis through ultrahigh-speed photography. Welding Journal research supplement, vol. 72, no. 3, pp.101s-106s.

Appendices

Appendix A-CDW raw data and parameters

Code	No	Tip Length (mm)	Drop Height (mm)	Capacitance (Farads)	Voltage (Volts)	Specimen Diameter (Inches)	Actual Welding Time(ms)	Welding Time (ms)	Strength (Mpa)
M11	53	0.5364	25.09	0.07	46.29	0.125	0.00109	0.00085	583.86
M11	54	0.5364	25.09	0.07	46.29	0.125	0.00101	0.00085	686.20
M11	68	0.5565	26.81	0.07	46.29	0.125	0.00123	0.00085	721.10
M11	90	0.5504	26.29	0.07	46.29	0.125	0.00118	0.00085	689.50
M12	8	0.5232	18.42	0.08	43.30	0.125	0.00109	0.00097	700.13
M12	51	0.5194	18.3	0.08	43.30	0.125	0.00131	0.00097	657.74
M12	73	0.5588	20.74	0.08	43.30	0.125	0.00121	0.00097	760.04
M12	80	0.5507	20.2	0.08	43.30	0.125	0.00133	0.00097	711.05
M13	1	0.5316	15.01	0.09	40.82	0.125	-	0.00109	787.54
M13	45	0.5334	15.01	0.09	40.82	0.125	0.00150	0.00109	651.58
M13	75	0.5525	16.09	0.09	40.82	0.125	0.00162	0.00109	747.30
M13	89	0.5588	16.42	0.09	40.82	0.125	0.00157	0.00109	741.84
M14	5	0.5161	23.41	0.07	75.59	0.25	0.00100	0.00085	631.06
M14	28	0.5093	23.1	0.07	75.59	0.25	0.00094	0.00085	649.74
M14	66	0.5410	25.48	0.07	75.59	0.25	0.00093	0.00085	669.10
M14	92	0.5375	25.18	0.07	75.59	0.25	0.00093	0.00085	648.19
M15	18	0.5159	17.96	0.08	70.71	0.25	0.00115	0.00097	643.16
M15	20	0.5253	18.56	0.08	70.71	0.25	0.00112	0.00097	698.65
M15	31	0.5156	18.1	0.08	70.71	0.25	0.00119	0.00097	626.45
M15	35	0.5347	19.15	0.08	70.71	0.25	0.0011	0.00097	667.61

Table A1. Screening experiment's raw data.

Code	No	Tip Length (mm)	Drop Height (mm)	Capacitance (Farads)	Voltage (Volts)	Specimen Diameter (Inches)	Actual Welding Time(ms)	Welding Time (ms)	Strength (Mpa)
M16	30	0.5575	16.36	0.09	66.67	0.25	0.00108	0.00109	652.04
M16	37	0.5585	16.41	0.09	66.67	0.25	0.00114	0.00109	629.24
M16	57	0.5347	15.17	0.09	66.67	0.25	0.00114	0.00109	629.31
M16	74	0.5537	16.16	0.09	66.67	0.25	0.00120	0.00109	590.72
M21	32	0.5491	30.98	0.07	60.00	0.125	0.00082	0.00078	74.39
M21	39	0.5387	30.1	0.07	60.00	0.125	0.00076	0.00078	127.09
M21	46	0.5347	29.6	0.07	60.00	0.125	0.00081	0.00078	158.60
M21	61	0.5425	30.5	0.07	60.00	0.125	0.00081	0.00078	151.97
M22	38	0.5491	23.95	0.08	56.12	0.125	0.00092	0.00089	36.35
M22	42	0.5464	23.72	0.08	56.12	0.125	0.00092	0.00089	23.44
M22	55	0.5588	24.68	0.08	56.12	0.125	0.00096	0.00089	91.77
M22	79	0.5347	22.8	0.08	56.12	0.125	0.00089	0.00089	39.15
M23	13	0.5464	18.7	0.09	52.92	0.125	0.00124	0.00100	39.18
M23	24	0.5464	18.7	0.09	52.92	0.125	0.00135	0.00100	271.73
M23	77	0.5334	17.91	0.09	52.92	0.125	0.00112	0.00100	30.06
M23	86	0.5367	18.1	0.09	52.92	0.125	0.00138	0.00100	290.52
M24	25	0.5415	30.31	0.07	97.10	0.25	0.00076	0.00078	294.76
M24	47	0.5349	29.7	0.07	97.10	0.25	0.00068	0.00078	273.16
M24	60	0.5525	31.42	0.07	97.10	0.25	0.00091	0.00078	273.99
M24	67	0.5484	31.01	0.07	97.10	0.25	0.00086	0.00078	288.60

Table A1. Screening experiment's raw data (continued).

Code	No	Tip Length (mm)	Drop Height (mm)	Capacitance (Farads)	Voltage (Volts)	Specimen Diameter (Inches)	Actual Welding Time(ms)	Welding Time (ms)	Strength (Mpa)
M25	21	0.5588	24.6	0.08	90.83	0.25	0.00111	0.00089	264.36
M25	44	0.5489	23.86	0.08	90.83	0.25	0.00106	0.00089	269.77
M25	59	0.5504	23.98	0.08	90.83	0.25	0.00103	0.00089	230.26
M26	9	0.5519	19.08	0.09	85.63	0.25	0.00116	0.00100	215.84
M26	11	0.5469	18.82	0.09	85.63	0.25	0.00115	0.00100	165.59
M26	36	0.5588	19.52	0.09	85.63	0.25	0.00117	0.00100	202.06
M26	84	0.5547	19.26	0.09	85.63	0.25	0.00120	0.00100	213.99
M31	15	0.5560	26.77	0.07	46.29	0.125	0.00114	0.00085	766.91
M31	22	0.5558	26.75	0.07	46.29	0.125	0.00112	0.00085	520.21
M31	27	0.5588	27.01	0.07	46.29	0.125	0.00112	0.00085	683.13
M31	95	0.5519	26.42	0.07	46.29	0.125	-	0.00085	767.28
M32	41	0.5509	20.22	0.08	43.30	0.125	0.00130	0.00097	530.00
M32	65	0.5588	20.74	0.08	43.30	0.125	0.00134	0.00097	653.07
M32	78	0.5509	20.22	0.08	43.30	0.125	0.00129	0.00097	781.74
M32	88	0.5499	20.15	0.08	43.30	0.125	0.00138	0.00097	829.77
M33	17	0.5583	16.4	0.09	40.82	0.125	0.00151	0.00109	650.92
M33	49	0.5583	16.43	0.09	40.82	0.125	0.00131	0.00109	826.83
M33	52	0.5540	16.07	0.09	40.82	0.125	0.00153	0.00109	804.62
M33	63	0.5540	16.17	0.09	40.82	0.125	0.00158	0.00109	751.59

Table A1. Screening experiment's raw data (continued).

Code	No	Tip Length (mm)	Drop Height (mm)	Capacitance (Farads)	Voltage (Volts)	Specimen Diameter (Inches)	Actual Welding Time(ms)	Welding Time (ms)	Strength (Mpa)
M34	29	0.5530	26.5	0.07	75.59	0.25	0.00095	0.00085	825.92
M34	40	0.5436	25.7	0.07	75.59	0.25	0.00096	0.00085	510.52
M34	70	0.5491	26.17	0.07	75.59	0.25	0.00110	0.00085	754.00
M34	93	0.5547	26.66	0.07	75.59	0.25	0.00106	0.00085	799.54
M35	26	0.5494	20.22	0.08	70.71	0.25	0.00113	0.00097	840.46
M35	34	0.5558	20.53	0.08	70.71	0.25	0.00113	0.00097	736.39
M35	72	0.5525	20.32	0.08	70.71	0.25	0.00110	0.00097	831.18
M35	85	0.5558	20.54	0.08	70.71	0.25	0.00106	0.00097	694.07
M36	19	0.5509	16.01	0.09	66.67	0.25	0.00129	0.00109	688.69
M36	43	0.5588	16.42	0.09	66.67	0.25	0.00139	0.00109	678.52
M36	58	0.5491	15.92	0.09	66.67	0.25	0.00133	0.00109	582.73
M36	96	0.5588	16.43	0.09	66.67	0.25	0.00096	0.00109	816.47
M41	16	0.5588	32.08	0.07	60.00	0.125	0.00107	0.00078	35.94
M41	23	0.5471	30.88	0.07	60.00	0.125	0.00132	0.00078	18.72
M41	33	0.5329	29.44	0.07	60.00	0.125	0.00124	0.00078	139.49
M41	87	0.5415	30.3	0.07	60.00	0.125	0.00129	0.00078	210.87
M42	2	0.5441	23.48	0.08	56.12	0.125	0.00132	0.00089	0
M42	7	0.5517	24.07	0.08	56.12	0.125	0.00141	0.00089	113.55
M42	64	0.5100	20.77	0.08	56.12	0.125	0.00112	0.00089	34.08
M42	91	0.5352	22.79	0.08	56.12	0.125	-	0.00089	25.86

Table A1. Screening experiment's raw data (continued).

Code	No	Tip Length (mm)	Drop Height (mm)	Capacitance (Farads)	Voltage (Volts)	Specimen Diameter (Inches)	Actual Welding Time(ms)	Welding Time (ms)	Strength (Mpa)
M43	6	0.5509	19.02	0.09	52.92	0.125	0.00169	0.00100	171.61
M43	62	0.5237	17.37	0.09	52.92	0.125	0.00169	0.00100	161.04
M43	83	0.5306	17.67	0.09	52.92	0.125	0.00154	0.00100	28.60
M43	94	0.5415	18.44	0.09	52.92	0.125	0.00134	0.00100	28.75
M44	12	0.5525	31.42	0.07	104.20	0.25	0.00095	0.00078	177.24
M44	48	0.5512	31.4	0.07	104.20	0.25	0.00095	0.00078	185.52
M44	50	0.5194	28.18	0.07	104.20	0.25	0.00096	0.00078	128.78
M44	56	0.5227	28.44	0.07	104.20	0.25	-	0.00078	146.98
M45	3	0.5580	24.58	0.08	97.47	0.25	0.00098	0.00089	152.60
M45	10	0.5443	23.5	0.08	97.47	0.25	0.00088	0.00089	92.47
M45	71	0.5298	22.38	0.08	97.47	0.25	0.00106	0.00089	96.37
M45	81	0.5245	21.98	0.08	97.47	0.25	0.00108	0.00089	113.49
M46	4	0.5547	19.26	0.09	91.89	0.25	0.00119	0.00100	68.036
M46	14	0.5527	19.13	0.09	91.89	0.25	0.00111	0.00100	128.58
M46	76	0.5311	17.81	0.09	91.89	0.25	0.00112	0.00100	57.80
M46	82	0.5309	17.79	0.09	91.89	0.25	0.00111	0.00100	77.79

Table A1. Screening experiment's raw data (continued).

Appendix B-CDW raw data and parameters (revised copper)

Code	No	Tip Length (mm)	Drop Height (mm)	Capacitance (Farads)	Voltage (Volts)	Specimen Diameter (Inches)	Actual Welding Time(ms)	Welding Time (ms)	Strength (Mpa)
M44	5	0.5474	36.35	0.07	104.20	0.25	0.00072	0.00072	314.06
M44	7	0.5474	36.35	0.07	104.20	0.25	0.00070	0.00072	316.02
M44	8	0.5423	35.74	0.07	104.20	0.25	0.00073	0.00072	316.72
M44	11	0.5634	38.20	0.07	104.20	0.25	0.00075	0.00072	329.65
M45	1	0.5342	26.76	0.08	97.47	0.25	0.00092	0.00082	270.94
M45	3	0.5306	26.45	0.08	97.47	0.25	0.00090	0.00082	190.93
M45	4	0.5474	27.98	0.08	97.47	0.25	0.00090	0.00082	256.84
M45	10	0.5207	25.58	0.08	97.47	0.25	0.00105	0.00082	191.89
M46	2	0.5583	22.53	0.09	91.89	0.25	0.00106	0.00093	264.45
M46	6	0.5128	19.34	0.09	91.89	0.25	0.00109	0.00093	296.88
M46	9	0.5634	22.9	0.09	91.89	0.25	0.00112	0.00093	215.52
M46	12	0.5712	23.48	0.09	91.89	0.25	0.00103	0.00093	211.31

Table B1. Additional screening experiment's raw data (for copper).

Appendix C- CDW raw data and parameters (magnesium and mild steel)

Code	No	Tip Length (mm)	Drop Height (mm)	Capacitance (Farads)	Voltage (Volts)	Specimen Diameter (Inches)	Actual Welding Time(ms)	Welding Time (ms)	Strength (Mpa)
M54	1	0.5507	33.80	0.07	55	0.25	0.00070	0.00075	100.52
M54	2	0.5342	32.00	0.07	55	0.25	0.00069	0.00075	99.54
M54	3	0.5400	32.60	0.07	55	0.25	0.00072	0.00075	112.10
M54	4	0.5403	32.61	0.07	55	0.25	0.00067	0.00075	119.51
M54	5	0.5342	32.00	0.07	55	0.25	0.00070	0.00075	94.15
M64	1	0.5461	25.91	0.07	75.59	0.25	0.00093	0.00085	699.99
M64	2	0.5537	26.54	0.07	75.59	0.25	0.00096	0.00085	707.21
M64	3	0.5512	26.42	0.07	75.59	0.25	0.00092	0.00085	619.91
M64	4	0.5334	24.89	0.07	75.59	0.25	0.00099	0.00085	688.77
M64	5	0.5385	25.27	0.07	75.59	0.25	0.00092	0.00085	712.98

Table C1. Validating model's raw data (for magnesium and mild steel).

Appendix D-Residual plot (%mean)

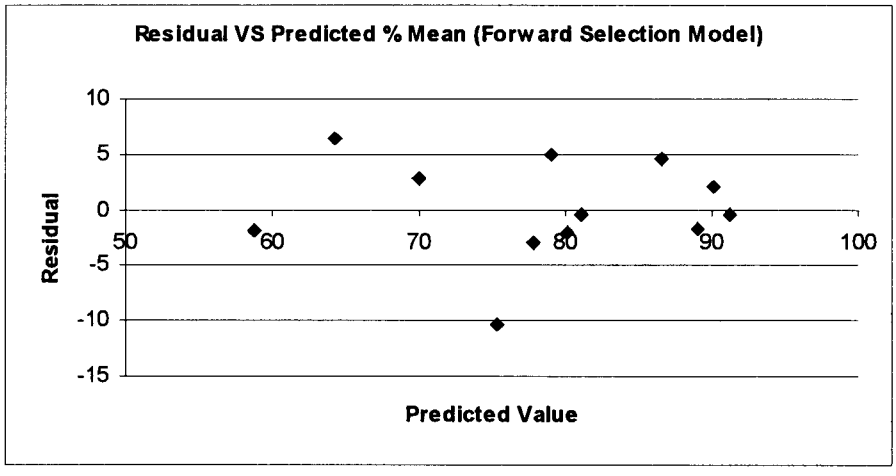

Figure D1. Residual plot (forward selection model for %Mean).

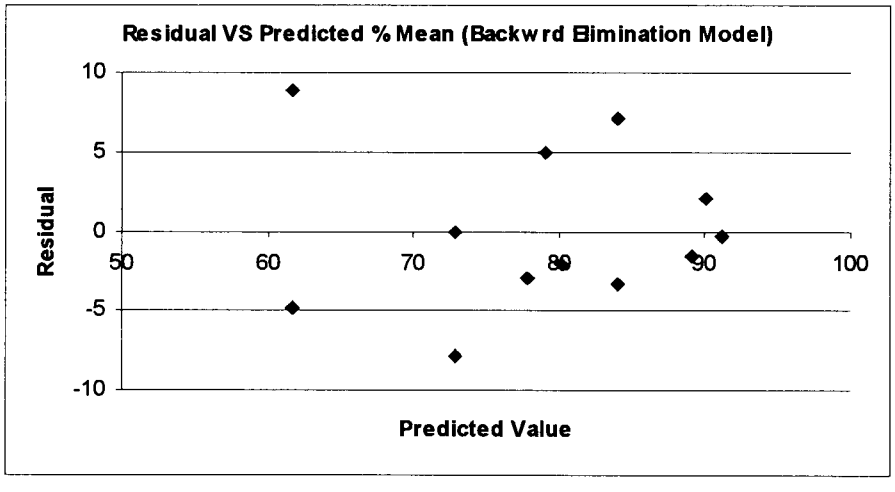

Figure D2. Residual plot (backward elimination model for %Mean).

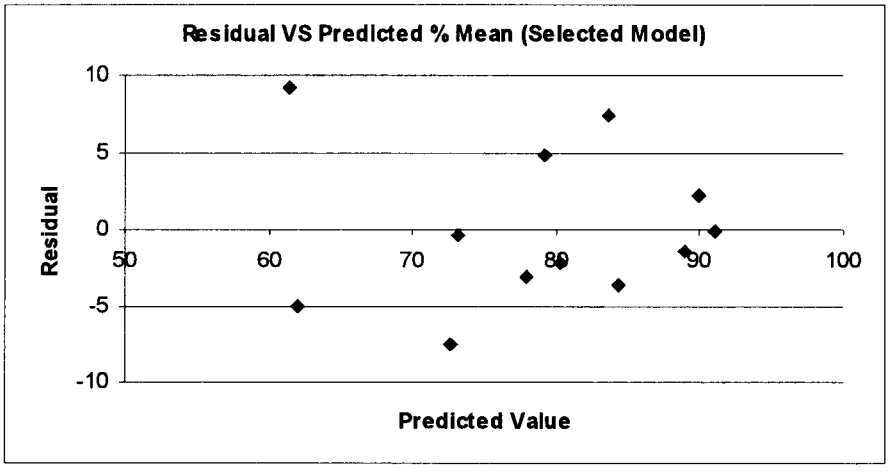

Figure D3. Residual plot (selected model for %Mean).

Appendix E-Residual plot (ln (%SD))

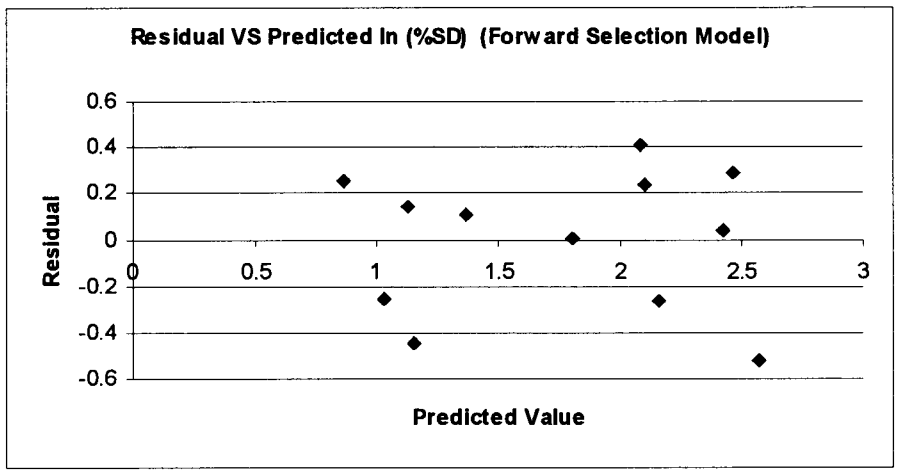

Figure E1. Residual plot (forward selection model for ln (%SD))

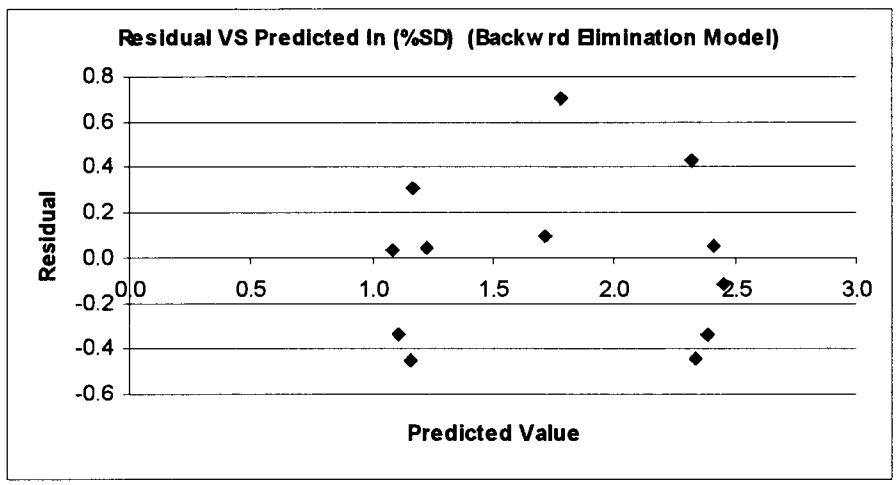

Figure E2. Residual plot (backward elimination model for ln(%SD))

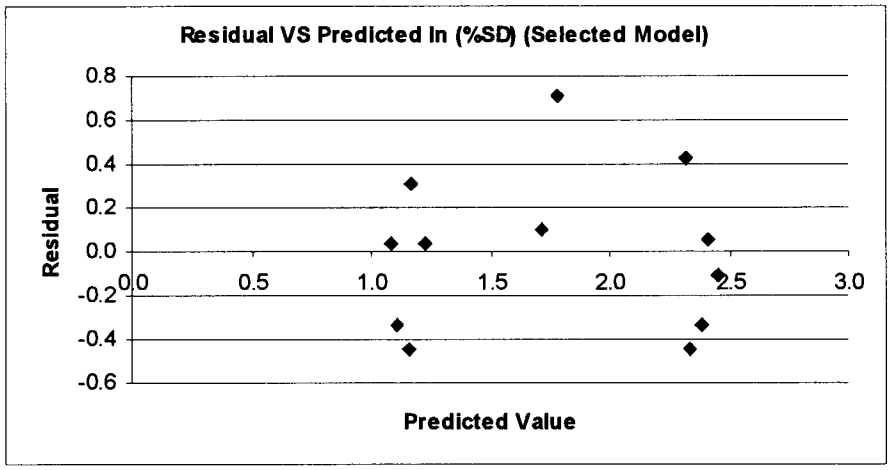

Figure E3. Residual plot (selected model).

Appendix F-Machining tip procedure

Machining tip procedure

1. Procedure requirements:

   1.1. Cathode material (workpiece)

   1.2. Dimension of ignition tip

   -Length (from process parameter calculation)

   -Diameter (typically 0.02")

   -Bevel angle (typically 2.5 degree)

2. Set up NC program.

   NC program was written by using the following format.

%

----N`-G`--X-`-----Z-`--F`--H

%

Where

N is a line number;

G is tool path;

X is X-axis coordinate;

Z is Z-axis coordinate;

F is feed;

M is machine language;

T is tool number;

The following is the CNC program

```
%
    N` G`  X `      Z `  F`  H`
    00 92   500       0
    01M03
    02 00   500 -    40
    03 00   328 -    40
    04 01     0 -    40  02
    05 00   500 -    40  02
    06 00   326 -    56  02
    07 01    20 -    50  02
    08 00   400      50  02
    09 00   326 -    68  02
    10 01    20 -    62  02
    11 00    50 -    40  02
    12 01     0 -    40  02
    13 00   500       0
    14M05
    13M30
%
```

3. Input command to NC machine for transferring NC program.

   3.1. Turn on NC machine by turning key to position I.

   3.2. Push H/C button to change to NC machine mode and then the NC program format is shown in the monitor.

   3.3. Push → button until highlight is in G position.

   3.4. Input G6 and then push input button twice.

4. Input NC program to computer.

   4.1. Execute Smart Cam program from SM6 directory. Enter "SC."

   4.2. After executing the SC program, choose "communication" menu.

   4.3. Choose "to machine" command.

   4.4. Push F1 button.

4.5. Insert disk with NC program into drive B.

4.6. Select drive B.

4.7. From drive B, select NC filename and then enter.

After that, the NC program will be transferred to NC machine.

5. Calibrate reference point of cutting tool.

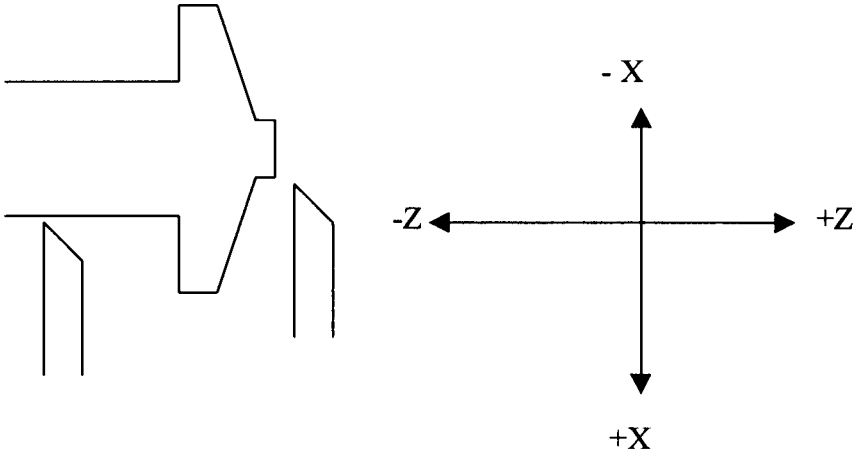

Figure F1. Calibrating reference point

According to the NC program, specification of tip of specimen relates to coordinate. Reference point, therefore, must be calibrated.

5.1 Calibrate X-axis reference.

5.1.1. Push H/C button to change to manual mode and select hand mode for moving cutting tool by hand.

5.1.2. Touch off on the diameter of the specimen with the cutting tool.

5.1.3. Set for X-axis by using DEL button.

5.1.4. Measure sample's diameter.

5.1.5. Move cutting tool in one half of the specimen diameter.

5.1.6. Set 0 for X-axis.

5.2. Calibrate Z- axis reference point.

5.2.1.Use shim for toughing off. Locate shim between tip and cutting tool.

5.2.2. Set 0 for Z-axis.

5.2.3. Since shim thickness is 0.006 inches, move cutting tool –0.006 inches in Z-axis.

5.2.4. Set 0 for Z axis.

5.3 Starting point of cutting tool.

In the NC program the starting point is X = 500 and Z = 500. However, X-axis in NC machine coordinate is shown in radial units. Consequently, the cutting tool must be set to coordinate X = 250 and Z = 500.

6. Making sample.

6.1. Push H/C button to change to NC mode and select NC mode for moving cutting tool by NC program.

6.2. Push start button.

6.3. Cutting tool is moved by following the command in NC program.

Appendix G-Loading dynamic graph procedure

Loading dynamic graph procedure

1. Load Quattro program by typing q in C prompt and then push enter.
2. Go to "filename" and choose directory A.
3. From "filename" choose "retrieve". The word " CDWG.WQ" will be shown.

Subsequently, push enter.

4. Push "Alt" and "A" simultaneously to select filename from directory A.
5. Select filename and enter.
6. After that, type title name in title box.
7. Push "Ctrl" and "Break" button simultaneously.
8. Go to "Graph" manu and select "name" and "Display"

    Display A shows graph Current and Voltage vs. Time.

    Display B shows graph Force and Voltage vs. Time.

    Display C shows graph Resistance and Voltage vs. Time.

    Display D shows graph Power and Voltage vs. Time.

Appendix H-CDW operating procedure

CDW Operating Procedure

1. Turn on a computer.
2. Set Date and time since CDW data filename is named by date and time.
3. Load data acquisition program by type "weldgaf" after c prompt.
4. Load anode and cathode into electrode holder.
5. Set height, voltage, and capacitance based on CDW equation.
6. Turn on 24 V power supply for operating relay switches.
7. Turn on 110 V power supply for charging to capacitor banks.
8. Before charging turn off TRIGGER button.
9. Put CHARGE button to charge electron to capacitor banks.
10. When the amp monitor of 110 V power supply show 0.01 A, put DROP button.
11. Welding is done, put TRIGGER button to on.
12. Make sure that no more charge in capacitor bank by shorting the circuit by screw-driver.
13. Move welding head to original position.
14. Unload specimen.

Appendix I-CDW efficiency estimation

CDW efficiency estimation

1. Efficiency can be calculated by using the following equation:

$$e = (\text{energy output}) \times 100 / (\text{energy input})$$

where e is CDW efficiency

2. Energy output is the area under the power and welding time curve, which is measured by using a pellimeter.

3. Energy input can be calculated from the following equation:

$$E_{input} = CV^2/2$$

where C is capacitance; and V is voltage

Appendix J-Statistical analysis of mean weld strength for first data

Statistical analysis of mean weld strength for first data

The following is the model from the backward elimination model

$$\% \text{ Mean} = 94.04 + 90.46\text{Gas} - 0.05\text{Ther} - 2.45\text{GasXTher} - 0.03\text{TherXTw} - 3.05\ \text{Tw}^2$$

where %Mean is the mean of the CD weld strength as a percentage of base material strength; Ther is thermal conductivity; Tw is welding time; and Gas is the percentage of gas content in the base material.

Table J1.The estimates of the coefficient in the multiple regression of %Mean on thermal conductivity (Ther); percentage of gas content in base material (Gas); and welding time (Tw) (backward elimination method).

Variable	Degree of Freedom	Estimate	Standard Error	T Statistic	P- Value
Intercept	1	94.0367	1.8657	50.4036	0.0001
Gas	1	90.4555	6.4876	13.9429	0.0001
Ther	1	-0.0477	0.0058	-8.2541	0.0002
GasXTher	1	-2.4535	0.1330	-18.4420	0.0001
TherXTw	1	-0.0289	0.0030	-9.7670	0.0001
Tw^2	1	-3.0475	1.4456	-2.1082	0.0796

From the analysis of variance in Table J1, there is evidence that regression of the %Mean on the percentage of gas content in the base material (Gas); thermal conductivity (Ther); the interaction term between the percentage of gas in the base material and thermal conductivity (GasXTher); the interaction term between thermal conductivity and welding time (TherXTw); and the quadratic term of welding time (Tw^2) can explain 99.43% of

the total variation in observes distance. The P-value of 0.001 in Table J2 shows that there is a significant relationship between the variables at a 99.9% confidence interval.

Table J2 . The analysis of variance for %Mean data (backward elimination method).

Source	Degree of freedom	Sum of Squares	Mean Square	F Statistic	P Value
Model	5	5883.6213	1176.7243	211.1727	0.0001
Error	6	33.4340	5.5723		
C total	11	5917.0553			

Appendix K-Statistical analysis of weld strength variability for first data

Statistical analysis of weld strength variability for first data

The following is the model from backward elimination method:

$$Ln(\%SD) = 1.1214 + 0.0009Ther + 0.2608Tw + 0.0374\ GasXTher - 0.642GasXTher$$

where ln(%SD) is the natural log of the standard deviatiom of CD weld strength as a percentage of base material strength; Ther is thermal conductivity; Tw is welding time; and Gas is the percentage of gas content in the base material.

Table K1.The estimates of the coefficient in the multiple regression of ln%SD on thermal conductivity (Ther); percentage of gas content in base material (Gas); and welding time (Tw) (backward elimination method).

Variable	Degree of Freedom	Estimate	Standard Error	T Statistic	P- Value
Intercept	1	1.1214	0.1586	7.0696	0.0002
Ther	1	0.0009	0.0004	2.1762	0.0660
Tw	1	0.2608	0.1103	2.3651	0.050
GasXTher	1	0.0374	0.0061	6.0855	0.0005
GasXTw	1	-0.6420	0.2985	-2.1507	0.0685

From the analysis of variance Table K1, There is evidence that the regression of ln(%SD) on thermal conductivity (Ther); welding time (Tw); the interaction term between percentage of gas content in the base material and thermal conductivity (GasXTher); and the interaction term between percentage of gas content in base material and welding time (GasXTw) can explain 86.26% of the total variation in the observed distance. However,

13.74% remains unexplained. the P-value of 0.0039 in Table K2 is less than 0.01. As a result, there is a relationship between the variables at a 99% confidence interval

Table K2 . The analysis of variance for %SD data (backward elimination method).

Source	Degree of freedom	Sum of Squares	Mean Square	F Statistic	P Value
Model	4	2.9536	0.7384	10.9857	0.0039
Error	7	0.4705	0.0672		
C total	11	3.4241			

Appendix L- Scatter plot

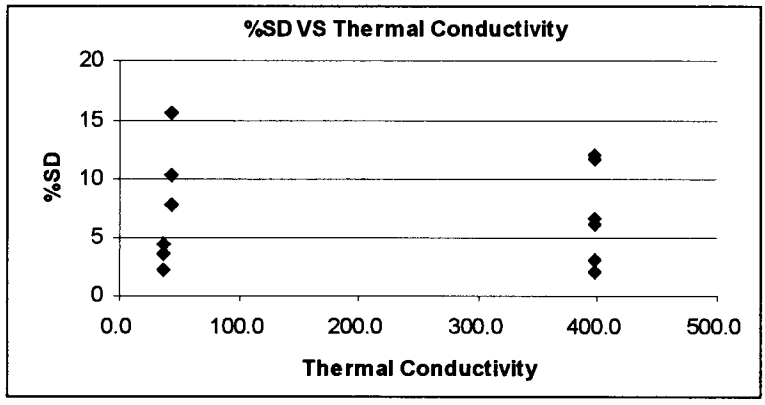

Figure L1. Scatter plot between %SD and thermal conductivity

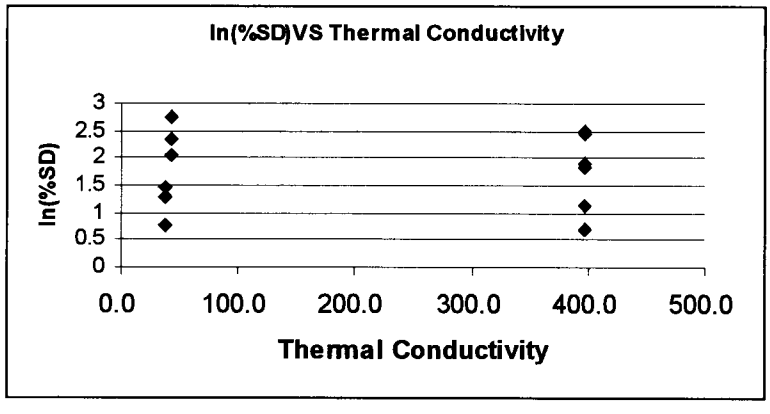

Figure L2. Scatter plot between ln(%SD) and thermal conductivity